Check for updates

Hollow carbon nanospheres: syntheses and applications for post lithium-ion batteries

Jin-Min Luo,†[ab] Yong-Gang Sun,†[ac] Si-Jie Guo,[ab] Yan-Song Xu,[ab] Bao-Bao Chang,[d] Chun-Tai Liu,[d] An-Min Cao [iD] *[ab] and Li-Jun Wan [iD] *[ab]

Hollow carbon nanospheres (HCNs) have found broad applications in different kinds of electrochemical storage devices. The characteristic hollow structure can endow carbon electrode materials with good reaction kinetics, high mechanical reliance against structural deformation, and powerful capability toward loading functional materials, which makes them particularly interesting for different energy storage systems. In this review, we summarize the recent progresses made in the research of HCNs, focusing on the synthesis strategies and corresponding applications as high-performance electrode materials in post lithium-ion battery (LIB) systems. Besides the widely implemented template-based routes, self-template routes based on the chemical design of polymeric precursors are also introduced. Efforts directed toward the shape evolution mechanism during synthesis, as well as the control capability of different methodologies on the key structural features of HCNs (such as shape, compositions, and architectures), will also be highlighted. Furthermore, we introduce the representative applications of the prepared HCNs in post LIBs, such as lithium–sulfur batteries, sodium-ion batteries, and potassium-ion batteries. We attempt to correlate the battery performance with the structural characteristics of HCNs so as to not only make good use of the advantage of shape control, but also facilitate understanding regarding the charge storage mechanism in the newly emerging technologies.

[a] CAS Key Laboratory of Molecular Nanostructure and Nanotechnology, and Beijing National Laboratory for Molecular Sciences, Institute of Chemistry, Chinese Academy of Sciences (CAS), Beijing 100190, People's Republic of China. E-mail: anmin_cao@iccas.ac.cn, wanlijun@iccas.ac.cn

[b] University of Chinese Academy of Sciences, Beijing 100049, People's Republic of China

[c] School of Chemistry & Chemical Engineering, Yancheng Institute of Technology, Yancheng, 224051, People's Republic of China

[d] Key Laboratory of Materials Processing and Mold, Ministry of Education, National Engineering Research Center for Advanced Polymer Processing Technology, Zhengzhou University, Zhengzhou, 450002, People's Republic of China

† J.-M. Luo and Y.-G. Sun contributed equally to this work.

Jin-Min Luo is a PhD student at the Key Laboratory of Molecular Nanostructure and Nanotechnology, Institute of Chemistry, Chinese Academy of Sciences (ICCAS). Her main research interests include controlling the surface of cathode materials for LIBs and designing the structure and components of anode materials for electrochemical energy storage.

Jin-Min Luo

Yong-Gang Sun is a Lecturer at the Yancheng Institute of Technology. He received his BS (2008) and MS (2014) in Chemistry from Soochow University and received his PhD from the Institute of Chemistry, Chinese Academy of Sciences, in 2018. His research interest is primarily concerned with the design and synthesis of nanostructured materials for energy storage and conversion.

Yong-Gang Sun

1. Introduction

Carbon species have found broad applications in the electrochemical field due to their unique properties such as chemical stability, high electronic conductivity, and tunable surface chemistry.[1] Typically, the success of graphite as the anode material of lithium-ion batteries (LIBs) has encouraged numerous research efforts on carbonaceous species for their applications as possible electrode materials in the field of batteries.[2] Different control strategies have accordingly been developed with regard to carbon to modulate its physicochemical properties in order to cater to the need of its electrochemical applications. As a specific category of carbon, hollow carbon nanospheres (HCNs) represent a successful example of structural control to circumvent the challenges when using it as the electrode material in batteries.[3] Such hollow structures have been known to benefit the electrochemical performance in different ways, such as good reservoir for electrolytes, designable carrier for active materials, flexible matrix against mechanical deformation, and preferred reactor for fast kinetics.[4] Accordingly, the engineering of carbon materials into different hollow architectures has become a widely used methodology toward the pursuit of high-performance electrode materials, particularly for systems plagued by large volumetric deformation as well as sluggish reactions kinetics: they can benefit from the inner void that can provide sufficient space for electrode expansion during the charge/discharge process.[5] Meanwhile, when compared with solid electrodes, the hollow structure shortens the conduction path and carbonaceous substrates promote conductivity; both these factors improve the overall rate performance of the batteries. For better electrochemical performance, HCNs with a porous shell and elemental doping have also been continuously developed.

Different synthesis protocols have been developed for forming an internal cavity in such carbon nanospheres. Two major protocols have been used, namely, a template-based one[6] and a template-free one;[7] they are differentiated by whether extra templates are borrowed for structural control. Template-based routes (TBRs) represent a straightforward solution to build an internal cavity by replicating the shape of the preexisting templates, which exist either as hard ones (such as the widely used SiO_2 species)[8] or surfactant-based soft ones.[9] TBR synthesis approaches have witnessed enormous success in the structural control of carbon species and can unfold the promising potential of HCNs in different fields.[10] However, they are also known for their shortcomings such as low yield, high cost, tedious operations steps, and limited capability in building structures with higher complexity and functionality. Therefore, recently, self-template processes (STPs)—also known as template-free synthesis approaches—have started to draw research attention with the potential to address the synthesis challenges faced by HCNs.[11] STPs focus on the chemical control of the prepared carbon precursor and can achieve a self-hollowing process without the use of additional templates, thereby providing alternative routes for HCNs via a possible scalable and facile route. Further, the synthesis of HCNs usually involves collaborative efforts rather than mere shape control, which can be associated with multiple aspects such as composition, configuration, and surface modification of the prepared HCNs toward the optimized performance in different applications.

Post LIBs are a collection of technologies that are considered to be alternative battery systems with higher potential for large-scale energy storage applications.[12] Due to the increased concerns for limited Li^+ resources on earth as well as lithium's uneven distribution, other secondary batteries that are based

An-Min Cao earned his PhD from the Institute of Chemistry, Chinese Academy of Sciences (ICCAS), in 2006. He worked in Prof. Gotz Veser's group in 2007–2010, investigating functional nanomaterials designated for catalytic reactions. Then, he worked at the University of Texas, Austin, on clean-energy-related materials with Prof. A. Manthiram. He has been serving as a Full Professor at ICCAS since 2012. His research currently focuses on developing advanced functional nanomaterials for secondary batteries and electrochemical catalytic reactions.

An-Min Cao

Li-Jun Wan received his BS and MS in Materials Science from the Dalian University of Technology in 1982 and 1987, respectively, and PhD in Materials Chemistry from the Tohoku University of Japan in 1996. He has been serving as a Full Professor at the Institute of Chemistry, Chinese Academy of Sciences (ICCAS), since 1999, and he served as the Director of ICCAS from 2004 to 2013. He was appointed as the President of the University of Science and Technology of China in 2015. His research focuses on the physical chemistry of single molecules and molecular assemblies, nanomaterials for applications in energy and environmental science, and scanning probe microscopy. In recognition of his research achievements, he has been selected as an Elected Academician of CAS and the Academy of Sciences for the Developing World (TWAS), as well as a Fellow of the Royal Society of Chemistry, UK.

Li-Jun Wan

on abundant metal ions, particularly K^+ and Na^+, have recently attracted increasing research attention.[13] The corresponding potassium-ion batteries (PIBs) and sodium-ion batteries (SIBs) share similar working mechanisms as that of LIBs, which makes them appropriate toward expanding the current knowledge for the facile development of post LIB technology; meanwhile, achieving higher energy density and lower cost can facilitate its applications.[14] Despite the fast growth, the development of such battery systems face challenges in the development of electrode materials that can be stable for extended cycles. Taking PIBs as the example, K^+ ions are much larger in size (1.38 Å $vs.$ 1.02 Å of Li^+); therefore, the intercalation/deintercalation process becomes susceptible to large volumetric deformations in the target electrode materials, particularly carbonaceous species as the most promising anode ones.[15] In this regard, it has become a prerequisite that electrode materials of PIBs can tolerate the destructive charge/discharge process to ensure stable electrochemical performance. From the design point view, engineering electrode materials into hollow structures is highly favorable due to their unique capability in combating structural deformations. Accordingly, HCNs-based anodes are drawing increased research attention in post LIB technologies to exploit its resilience against mechanical failures.

There have been some excellent reviews regarding the synthesis and applications of HCNs for different areas.[3d,16] In this review, we will initially update on the recent progresses made in the synthesis approaches for HCNs. Special attention will be paid toward its shape control mechanism, according to which a reliable hollowing effect can be ensured and precise control can be achieved over the morphological parameters. These newly developed STPs will also be highlighted due to their promising potential in providing the scalable synthesis capability for further applications. Meanwhile, we will discuss the unique capability of HCNs as anode materials for post LIB technologies. Different battery systems such as lithium–sulfur (Li–S) batteries, SIBs, and PIBs will be introduced with a focus on the contributions from their hollow characteristic. We demonstrate that structural engineering is highly effective in addressing the stability issue plaguing these post LIB technology; further, there is promising potential to integrate other control strategies, particularly compositional control, to achieve both high reversible capacity and high cycling stability for post LIB technologies. Finally, we conclude this review by proposing our considerations of the present challenges and perspectives related to the development of HCNs in the energy storage field.

2. Synthesis protocols for HCNs

The creation of a cavity inside nanospheres requires the existence of a spherical object with the desired internal complexity such that the selective removal of the inner portion can become possible. Therefore, the fabrication of such a precursor with core–shell-type configuration has become imperative in synthesis design. Currently, there exist two main approaches to achieve this goal. First, template-assisted syntheses use chemically different particles as the seeds such that targeted carbonaceous species can be grown around, thereby forming a typical core–shell structure with two different kinds of species suited for the creation of hollow structures.[17] Second, STPs focus on the growth control of the carbonaceous precursors synthesized into an inhomogeneous state whose inner difference could be investigated and revealed by using a suitable etching agent.[18] Seemingly easy, intricate control over the chemical properties during growth control in the STP process makes the creation of HCNs a challenging task. Below, we update the recent growth in the reported synthesis protocols with a focus on the shape control capability and hollowing mechanism.

2.1 TBRs

Depending on the different kinds of templates used during synthesis, TBRs can be briefly classified into two major types: hard template and soft template. Below, we will summarize the recent progresses made in the TBRs, paying special attention to their diverse structures and functionalities that are important to battery applications.

2.1.1 Hard-template synthesis. Hard-template-based synthesis relies on the use of sacrificial solid nanoparticles, particularly SiO_2 nanospheres, which could be facilely prepared via the Stöber process.[19] A nanocasting operation is necessary to replicate the shape of the seeds, which typically include the surface deposition of carbonaceous species around the preexisting templates to form a core–shell-type structure. Hard-template-based synthesis can provide a reliable protocol for the creation of hollow structures; moreover, it has become the most used tool by materials scientists for the synthesis of HCNs. Several excellent reviewers have investigated this synthesis topic.[20] In particular, Jaroniec $et~al.$ discussed the construction of HCNs with the pore structure designed on the molecular-lever base, which highlighted the complicated interactions between the carbonaceous precursors with the template materials.[21]

Along with the fast development of HCNs, the synthesis efforts were not only focused on the construction of hollow features in a uniform and controllable way, but also exerted to achieve comprehensive control over the targeted products in order to maximize their potential for specific applications. Accordingly, template-based synthesis is usually integrated with other control efforts, particularly compositional design, to produce complicated systems with multifunctional benefits. Lou $et~al.$ carried out a systematic study on the construction of hollow nanocomposites with different kinds of materials introduced for specific functions.[22] A recent progress made in this topic is related to the synthesis of a SnS_2@HCNs composite, where SnS_2 species were present inside the carbon wall.[23] A typical hard-template route was adopted to build such a structure, as shown in Fig. 1. SiO_2 nanospheres were initially built as the substrate; then, SnO_2 was coated onto its surface, forming the SiO_2@SnO_2 core–shell structures. The subsequent carbon coating was achieved by the polymerization of dopamine, forming a polydopamine (PDA) nanolayer as the outer shell. The selective etching of SiO_2 corresponded to the cavity formation inside the nanospheres, while the SnS_2 species
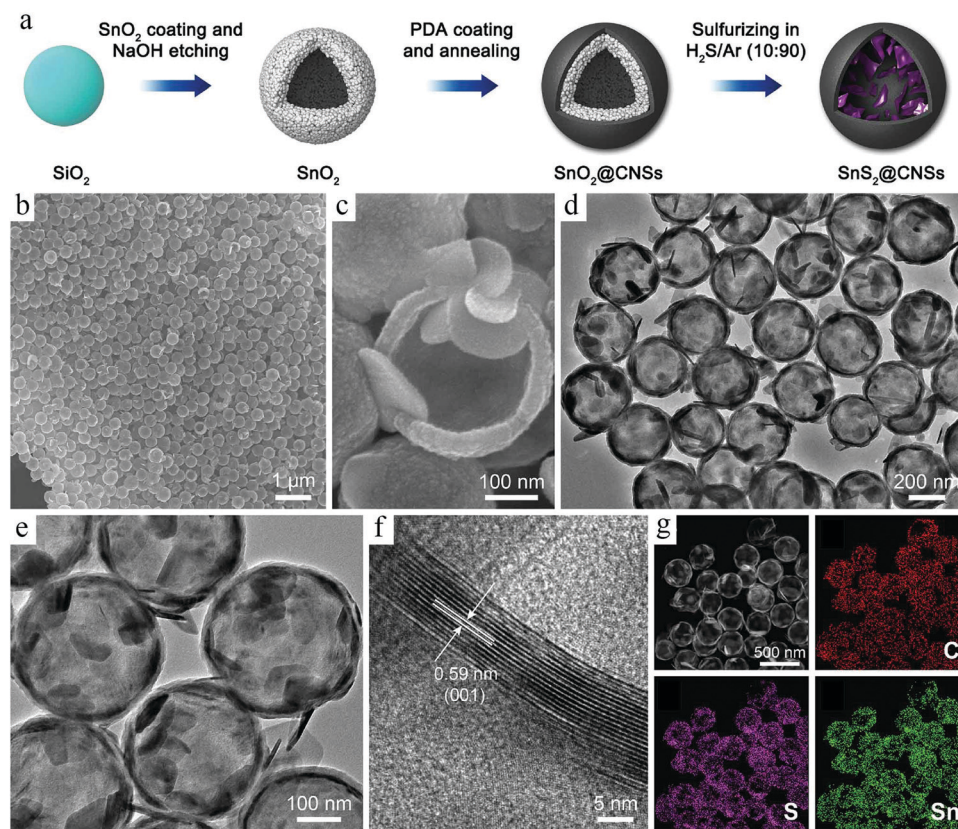
Fig. 1 (a) Schematic illustration of the synthesis processes of SnS$_2$@CNSs. (b and c) Field-emission scanning electron microscopy (FESEM) images, (d and e) TEM images, and (f) high-resolution transmission electron microscopy (HRTEM) image of SnS$_2$@CNSs. (g) High-angle annular dark-field scanning transmission electron microscopy (HAADF-STEM) image of SnS$_2$@C hollow nanospheres and corresponding elemental mapping images. Reproduced with permission.[23] Copyright 2018, Elsevier.

were produced *via* a high-temperature sulfidation process. Transmission electron microscopy (TEM) analysis confirmed the formation of hollow structures. The coexistence of electrochemically active SnS$_2$ and electronically conductive carbon in this nanocomposite made it a good model system to study the morphological effects on the electrode materials, which facilitate the programmable capability provided by the hard-template-based synthesis process.

Considering the fact that multistep operations are needed to achieve structural control in hard-template-based synthesis, researchers have started to simplify the experimental procedure by using particles generated *in situ* as the seeds for subsequent surface coating.[24] The so-called *in situ* template routes usually include two reactions where the product from the first reaction can be directly used as the sacrificial template for the subsequent coating reaction. In this way, the tedious process related to the creation of the template can be saved to achieve a highly efficient route. For example, Yu *et al.* developed a mixed Stöber system, where silica formation and polymerization process can occur together.[24a] Silica alone was at the center (core), while a composite of silica and PDA also existed in the core. The success of this synthesis route is partly because of the fact that these two involved reactions can occur under similar alkali-catalyzed conditions, thereby making it possible to modulate

the growth behavior of both silica and PDA to form the desired structure (Fig. 2). The silica formed *in situ* can be readily removed for the construction of hollow mesoporous carbon spheres (HMCSs).

SiO$_2$ is usually considered to be the shape control agent for the creation of the inner cavity. Further, functional materials with specific functions can be used as the seeds to play a multifunctional role in the prepared composites. A representative example is the construction of sulfur@polyaniline (PANI) yolk–shell nanocomposite, where sulfur was used as the template as well as the active material for Li–S batteries. Zhou *et al.* were the first to prepare sulfur nanospheres, and then PANI was deposited around the S particles to form the shell, which is electronically conductive in nature.[25] The subsequent heating treatment could partially remove the inner sulfur to create the yolk–shell structure (Fig. 3), whose cavity could effectively alleviate its structural deformation when used as a cathode material in Li–S batteries. A recent research showed that it was possible to use the Ni particles generated *in situ* not only as a hard template to create the cavity, but also as a catalyst to facilitate the crystallization of the surface carbon at higher temperatures, featuring a dual role played by the inner template species.[26]

TBR necessitates the controlled deposition of carbon species around the preexisting seeds, which form a surface layer

2286 | *Mater. Chem. Front.*, 2020, **4**, 2283–2306

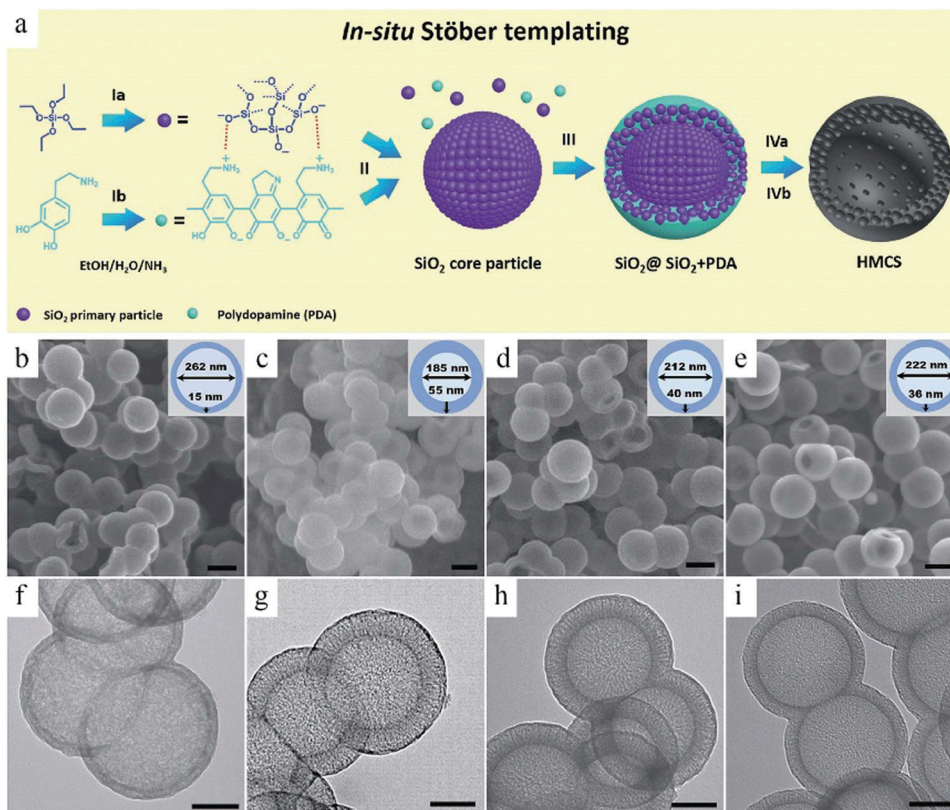This journal is © The Royal Society of Chemistry and the Chinese Chemical Society 2020

Fig. 2 (a) Schematic illustration of the *in situ* Stöber templating of HMCS. (b–e) SEM and (f–i) TEM images of HMCSs with different core–shell sizes for different concentrations and addition times of dopamine. Reproduced with permission.[24a] Copyright 2016, Royal Society of Chemistry.
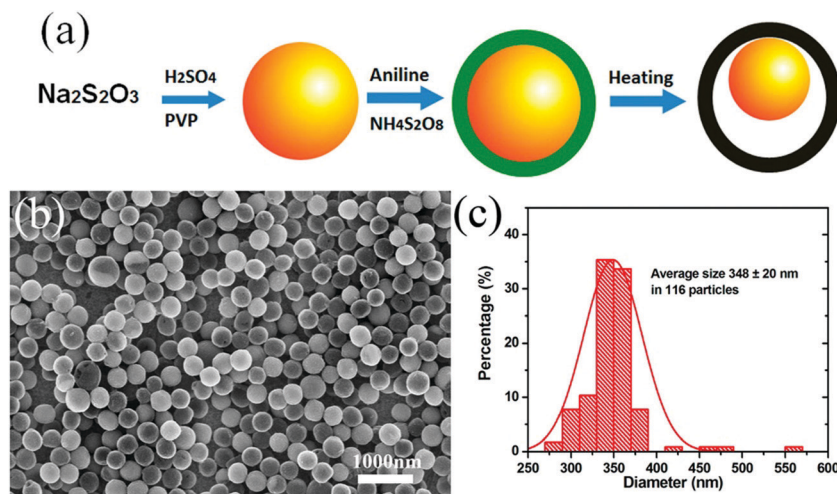

Fig. 3 (a) Two-step synthesis route for the S–PANI composite; the yellow sphere represents sulfur; dark green shell, PANI; and black shell, vulcanized PANI. (b) SEM images of the S–PANI core–shell composite using H_2SO_4 as the acid source and (c) the particle size distribution. Reproduced with permission.[25] Copyright 2013, American Chemical Society.

exhibiting a core–shell-type structure. Although the main goal of such a synthesis process is to produce a nanoshell, it is interesting to note that the formation of polymeric species also modifies the surface properties of the preexisting particle; this phenomenon can be exploited to fabricate complicated structures. For example, Cao *et al.* developed a polymerization-assisted coassembly process to create hierarchical structures.[27] The polymerization reaction between hexachlorocyclophosphazene and 4,4′-sulfonyldiphenol formed the poly(cyclotriphosphazene-*co*-4,4′-sulfonyldiphenol) (PZS) polymer, which was deposited on the SiO_2 seeds. It was interesting to observe that the reaction of PZS could also initiate the further assembly of SiO_2 particles,

This journal is © The Royal Society of Chemistry and the Chinese Chemical Society 2020

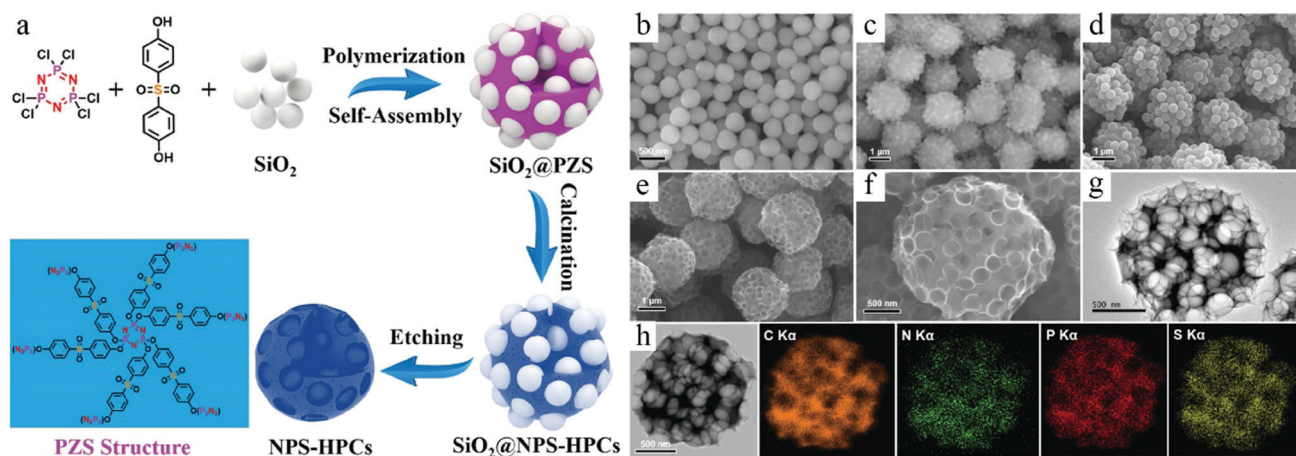*Mater. Chem. Front.*, 2020, **4**, 2283–2306 | **2287**

Fig. 4 (a) Schematic illustration for preparing nitrogen, phosphorus, and sulfur codoped hierarchical porous carbon spheres (NPS-HPCs). SEM images of (b) SiO$_2$ NPs, (c) self-assembly of SiO$_2$@PZS, (d) SiO$_2$@NPS-HPCs, and (e and f) NPS-HPCs. (g) TEM image of NPS-HPCs. (h) Energy-dispersive X-ray spectroscopy (EDS) mapping images of NPS-HPCs. Reproduced with permission.[27] Copyright 2018, American Chemical Society.

forming SiO$_2$@PZS composite microspheres probably due to the crosslinked reaction between the surface PZS species. Each microspheric particle existed as the aggregation of the core–shell-structured nanoparticles, exhibiting a hierarchical structure due to the coassembly process of SiO$_2$ and PZS (Fig. 4). The removal of SiO$_2$ and the subsequent carbonization process form a super-structure featuring pores of different lengths. In addition to the formation of a hierarchical structure, it should be noted that this work highlighted the promising potential of compositional control *via* the rational design of the polymerization process. The selection of PZS as the polymeric precursor for HCNs could enable the use of doping elements such as N, P, and S (NPS), whose existence in the carbon structures have been widely acknowledged as an effective method to modify the physico-chemical properties of HCNs for their advanced applications.[28]

2.1.2 Soft-template-based synthesis. Instead of using a solid object as the seeds for further growth, soft-template routes usually rely on surfactant-based micelles for cavity control. The creation of a hollow structure usually entails an effective organic–organic interaction between the carbon precursor and micelle templates for a stable self-assembly process, which is a challenging task particularly considering the unstable interface of micelle droplets during the polymerization of the carbon precursor.[29] It is, therefore, expected that the HCNs produced from soft templates are not as uniform as the ones prepared by using hard templates. Meanwhile, the available soft templates are also known to be limited and not as versatile as hard templates. However, an obvious advantage related to the soft-template process is the easy removal of templates, which could be achieved by simple operations (such as solvent wash or high-temperature treatment).

Wu *et al.* reported a facile soft-template synthesis route for the construction of HCNs, which comprised the use of Triton X-100 as the surfactant to form micelles, while a conjugated polymer generated *in situ* was used as the carbon precursor.[3b] As shown in Fig. 5, Triton X-100 formed micelles in the solution, and the two monomers used for polymerization,

namely, aniline and pyrrole (which have different hydrophobic properties), existed at different locations in the micelles. Copolymerization occurred upon the addition of catalyst because of which the two kinds of monomers diffused to the micelle–water interface. It was considered that the conjugated polymer was sufficiently robust at the interface to be grown into nanospheres and successfully prevented the collapse of the micellar structure. The subsequent heat treatment could facilely remove the thermally decomposable Triton X-100, leading to the formation of HCNs with sizes smaller than 100 nm. It should be noted that such a small size is usually difficult to achieve *via* the soft-template route. The micelle became much more unstable and easier to grow due to thermo-dynamic driving. The authors highlighted the importance of careful design on not only the copolymer precursor to form mechanically stable particles, but also the subsequent thermal conditions to transform the copolymer into hard carbon without destroying the hollow structure.

The lack of strong support as solid particles facilitated the formation of surface polymeric species, which increased the uncertainty and instability in the shape control for soft-template syntheses. On the other hand, the critical role played by the organic–organic interactions made it possible to take full advantage of the rich knowledge base of organic chemistry to achieve systematic control over the key structural features related of the formed micelles, *e.g.*, mesopores. Since a long time, Zhao *et al.* focused on the design and control of nanoemulsions as well as their assembly for the construction of mesoporous carbon structures.[30] For example, recently, they used organic molecules such as 1,3,5-trimethylbenzene (TMB) to modify the state of nanomicelles prepared by the Pluronic F127 surfactant.[17b] They concluded that the selection of such an organic additive could not only affect the formation of the nanoemulsion, but also play a critical role in modulating the interaction between the nanomicelles and surface carbon precursors, particularly PDA formed through an *in situ* growth process, accordingly leading to the formation of hollow
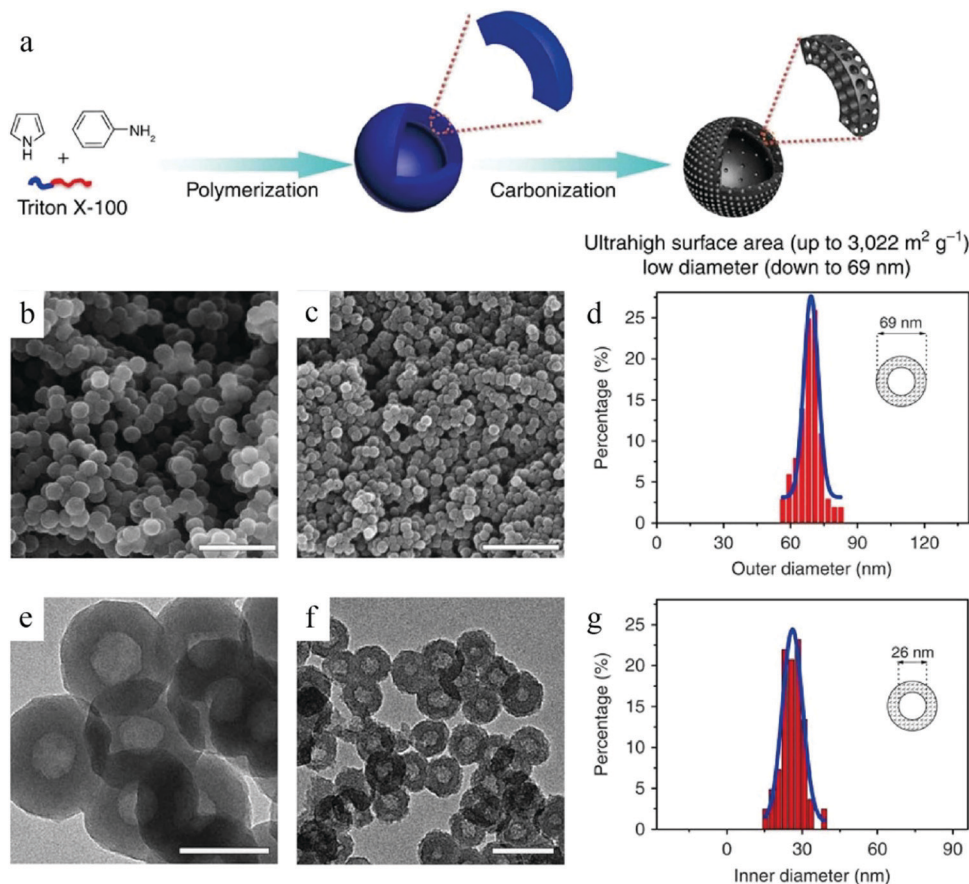
2288 | *Mater. Chem. Front.*, 2020, **4**, 2283–2306

This journal is © The Royal Society of Chemistry and the Chinese Chemical Society 2020

Fig. 5 (a) Schematic illustration of the preparation of HCNs. SEM images of (b) polyaniline-*co*-polypyrrole (PACP) and (c) HCN-900-20H2R. TEM images of (e) PACP and (f) HCN-900-20H2R. Histograms of the (d) outer and (g) inner diameters of HCN-900-20H2R as per the analyses of the SEM and TEM images, respectively. Reproduced with permission.[3b] Copyright 2015, Nature.
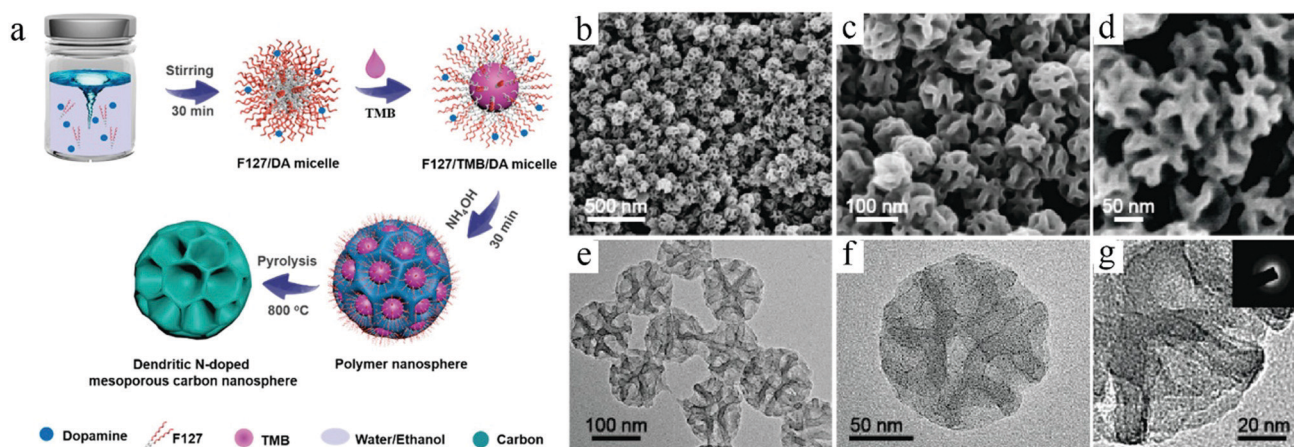

Fig. 6 (a) Synthesis procedure for the dendritic N-doped mesoporous carbon nanospheres prepared by the versatile nanoemulsion assembly approach. (b–d) SEM and (e and f) TEM images of the dendritic N-doped mesoporous carbon nanospheres with ultralarge pore size prepared by the versatile nanoemulsion assembly approach. Reproduced with permission.[17b] Copyright 2019, American Chemical Society.

structures with flexible control over the cavity and pores (Fig. 6). A detailed discussion on the creation of ordered pores inside the carbon structures could be found in a recent review paper published by Zhao's group, which features the flexibility and

effectiveness of the soft-template routes in fabricating multi-level architectures and functionalities.[30b]

The unstable interface in the soft-template routes makes it usually suitable for the polymeric precursor, whose flexible

This journal is © The Royal Society of Chemistry and the Chinese Chemical Society 2020

Mater. Chem. Front., 2020, **4**, 2283–2306 | **2289**

structure and rich functional groups facilitate the formation of a relatively stable micelle–polymer interface for structural control. Recent progresses made in soft-template routes demonstrated the possibility of expanding this synthesis protocol to other carbon precursors such as biomass[31] and fullerenes.[32] Typically, Chen *et al.* could fabricate a large variety of hollow fullerene nanostructures by using xylene as the template molecule and C_{60} as the shell materials for interface growth.[32] The authors identified that the deformation of the liquid micelle promised unique capability to form interconnected particles: the material exchanged between the micellar droplets could form channels in the wall of the micelles, which were transformed into bottleneck structures upon the controlled deposition of C_{60}. Multicompartment nanocontainers with interconnected hollow structures could be effectively produced in a controllable manner (Fig. 7), revealing the unique ability of structural control facilitating the liquid nature of the soft template.

2.2 STPs

The synthesis routes for HCNs with the assistance of different templates provided a designable and straightforward method to create a hollow cavity, which relies on the fact that the template materials are inherently different from the surface carbon materials. Despite the effectiveness of shape control, the limited yield as well as tedious operation procedures impeded their further applications. Accordingly, STPs, also known as template-free routes, have drawn increasing research

attention in the hope of obtaining scalable synthesis capability to assert the potential of HCNs.

In the absence of shape-directing templates, the creation of hollow structures need to rely on the carbon precursors themselves. It has, therefore, become necessary to effectively control the physicochemical properties of the formed carbon precursors during the hollowing process. Inspired by the soft-template process, researchers have started to explore the possibility of using carbon precursors as surfactants, too, for the formation of micelles. This attempt has been encouraged by the fact that several polymers are amphiphilic in the presence of different functional groups, such as carboxyl and hydroxyl groups. Recently, Du *et al.* demonstrated such a STP process for HCNs by using polyamic acid (PAA) as the carbon precursor as well as a surfactant for micelles.[33] As shown in Fig. 8, PAA polymers were prepared in solution *via* a stepwise polymerization reaction between two monomers, namely, pyromellitic dianhydride (PMDA) and 4,4′-oxydianiline (ODA), forming the PAA polymers. They were considered to directly form vesicles in solution due to their amphiphilic nature, leading to a facile synthesis process for the creation of hollow structures.

The essential role played by the carbonaceous precursors indicated the promising potential of their chemical design in creating hollow structures without the necessity of additional templates. Combined with solvent selection, it has become possible to achieve systematic control over the self-assembly processes of the polymeric precursors, accordingly forming
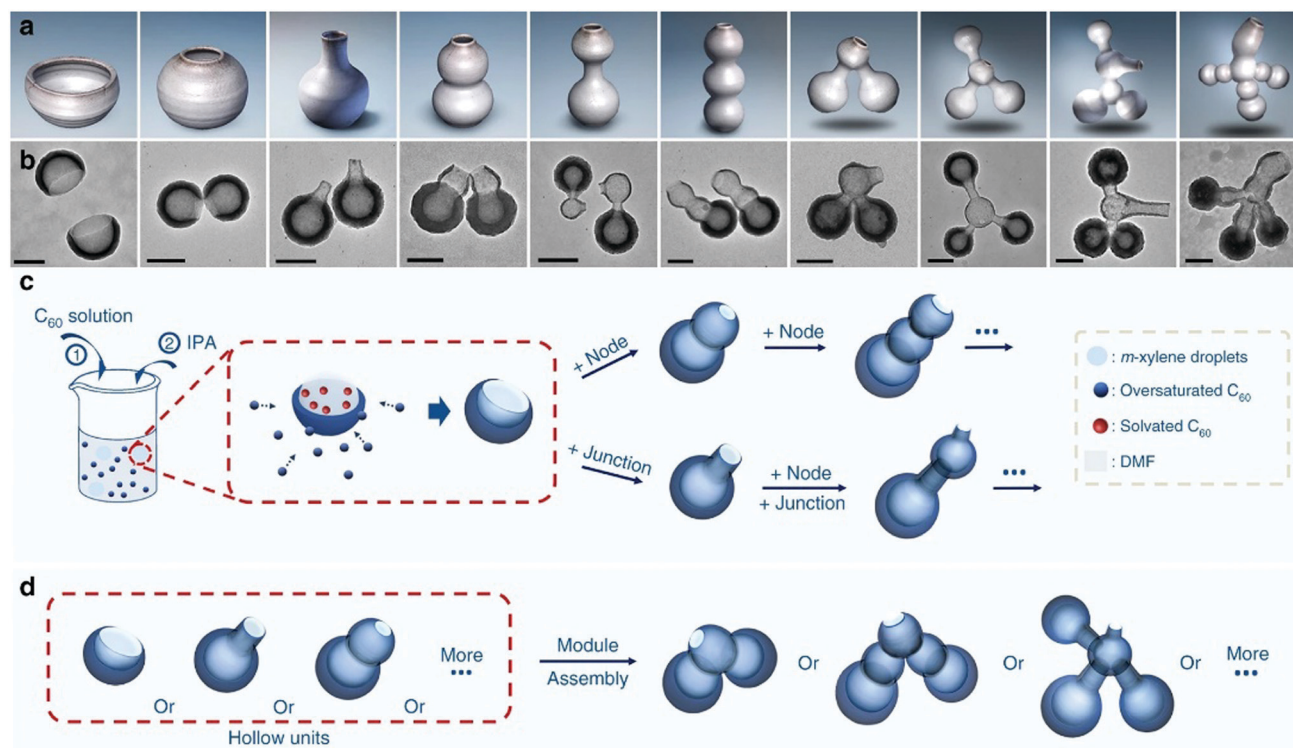

Fig. 7 Schematic illustrating the concept and design. (a) Models of pottery and (b) TEM images of their corresponding nanostructures created with nanopottery. (c) Schematics illustrating the synthesis of different hollow units and (d) connections between the hollow units. Reproduced with permission.[32] Copyright 2019, Nature.
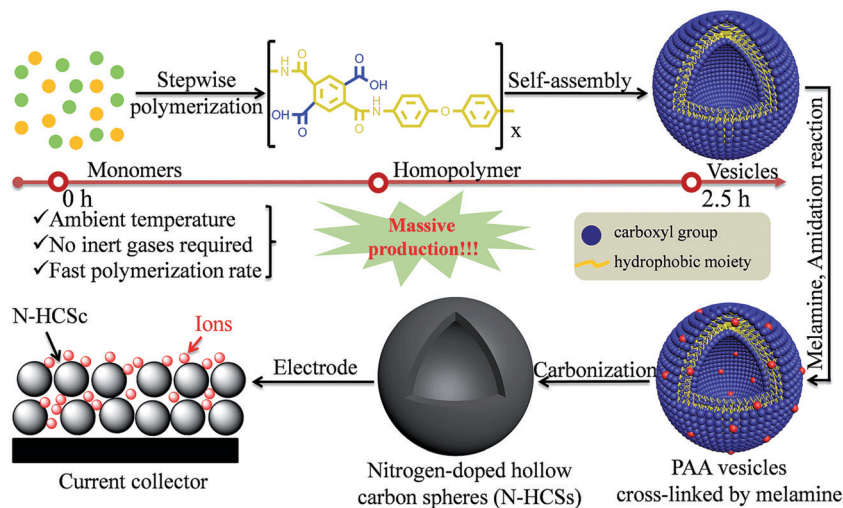
Fig. 8 Scalable fabrication of PAA homopolymers and their subsequent self-assembly into vesicles as well as carbonization into nitrogen-doped hollow carbon spheres (N-HCSs). Reproduced with permission.[33] Copyright 2016, Royal Society of Chemistry.

nanostructures with different pore structures. For example, Qiao *et al.* worked on the self-assembly of poly(ethylene oxide)-*b*-polystyrene (PEO-*b*-PS) to modulate its structures in different solvents.[34] The authors found that this block polymer could assemble into different structures (Fig. 9) when the polarity of the solvent was changed. By using a combination of formaldehyde dimethyl acetal (FDA)/1,2-dichloroethane (DCE) as the solvent, whose polarity can change in response to its binary compositions, PEO-*b*-PS assumed different shapes in the formed micelles. The subsequent reaction *via* the Friedel–Crafts reaction path could crosslink the polymers into robust porous polymers in which the micellar structures were effectively preserved for the creation of hollow characteristics. Tiny hollow carbonaceous structures with the inner cavity (size: ∼6.5 nm) could be achieved by means of the self-assembly process of PEO-*b*-PS, which played the dual role of surfactant as well as reactant; therefore, the hollow structure could not only be created, but also be retained through its crosslinking reaction, showing the capability to mimic a soft-template process while not requiring any additional surfactants.

Researchers have tried to explore new synthesis mechanisms for HCNs so as to break the strict limitations over the multi-functional roles played by the polymeric precursors. The success of template-assisted synthesis suggested that the particles should

be different in the center so that the core materials could be selectively removed to create the desired hollow structures. Recent progresses demonstrated that polymeric particles them-selves could be synthesized into the core–shell-type architecture, where the inner part is different in molecular weight when compared to the outer shell. For example, Wan *et al.* identified that 3-aminophenol-formaldehyde (3-AF) resin nanospheres formed in an aqueous solution could be inhomogeneous inside despite their unique morphology.[35] The authors carried out systematic control over the polymerization reaction and found that the particles showed a large variety of configurations as the inner molecular weight distribution was considered. Typically, 3-AF nanospheres could be synthetized into the core–shell type with reference to molecular weight (Fig. 10), where the inner part existed as oligomers with a much lower molecular weight as compared to the high-molecular-weight ones at the outer shell. The authors demonstrated that the self-acceleration nature of the polymerization reaction as well as control over the growth kinetics together determined the distribution of the polymeric species, accordingly leading to complicated but tunable con-figurations inside the particles. For the core–shell-type particles, a quick wash by a suitable solvent (acetone as identified by the authors) could selectively dissolve the inner oligomeric 3-AF species to form the cavity. The synthesis process was proven to
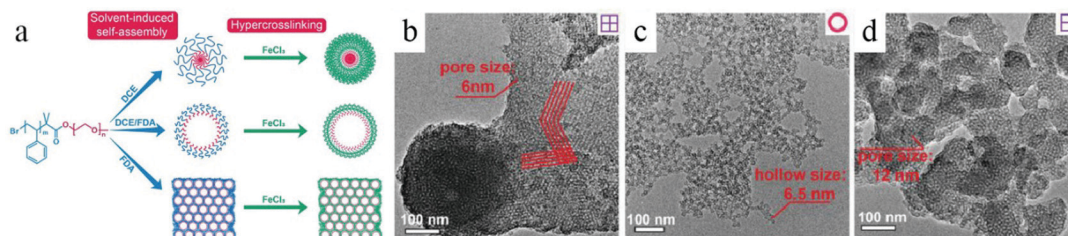

Fig. 9 (a) Synthesis route of hypercrosslinked polymers (HCPs) with different morphologies. TEM images of mesoporous bulk HCPs synthesized with (b) PEO45-*b*-PS190, (c) HCPs synthesized with PEO45-*b*-PS190, and (d) mesoporous bulk HCPs synthesized with PEO117-*b*-PS307. Reproduced with permission.[34] Copyright 2019, Wiley-VCH.
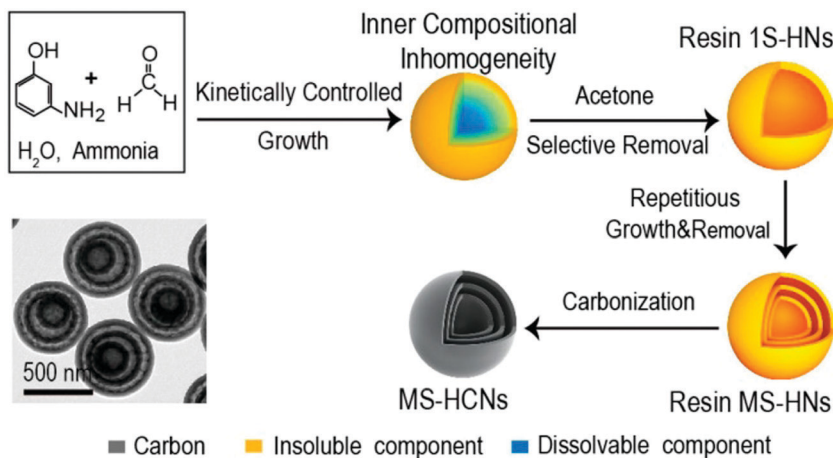
This journal is © The Royal Society of Chemistry and the Chinese Chemical Society 2020

Mater. Chem. Front., 2020, **4**, 2283–2306 | **2291**

Fig. 10 Schematic of the synthesis route for hollow 3-AF structures. Reproduced with permission.[35] Copyright 2017, American Chemical Society.

be highly reliable and could be expanded to construct complicated structures, particularly multishelled structures, with precise control over the morphological characteristics. In a recent research paper, the same group confirmed that such a synthesis route could be applied to other carbonaceous species (*e.g.*, coordination polymers), which were built into nanospheres with inner inhomogeneity suited for the facile production of hollow structures.[36]

The inhomogeneous nature of particles has been mostly discussed with regard to SiO$_2$.[37] Recent developments regarding detailed investigations on particle chemistry have revealed that such a phenomenon may exist for a large variety of materials, which accordingly provide an efficient tool for the creation of hollow structures. Interestingly, Huo *et al.* found that the newly formed nanocrystals of metal–organic frameworks (MOFs) could also show such inner structural complexity, which is contrary to the old wisdom that MOF crystals are considered to be homogenous in nature.[38] By using 1,4-benzene dicarboxylic acid (H$_2$BDC) as the linker and chromium ions as the metal source, the authors were able to fabricate solid MOF crystals *via* a hydrothermal process. The authors found that the core materials

are more vulnerable against etching by acetic acid, and they could be selectively removed to form a hollow structure without the assistance of any additional template materials (Fig. 11). Such a STP purely relied on the physicochemical properties of the MOF nanocrystals themselves, whose inner vulnerability was considered to be related to the fast formation of less-crystallized species during the initial nucleation stage, thereby forming a defect-rich core that could be selectively removed. Taking advantage of this new knowledge, the authors could fabricate highly crystalline multishelled MOFs with precise control over the shape parameters suitable for their applications.

The above-discussed syntheses demonstrated the possibility of creating the desired inner complexity by working on nanoparticles composed of a single component. However, from the synthesis point of view, it is reasonable to expect that a multicomponent characteristic can become more convenient to facilitate the core removal process. In this regard, Lu *et al.* designed a reaction system where two polymerization processes existed in the formed nanospheres.[39] The fast polymerization between *m*-phenylenediamine and diaminobenzoic acid started the precipitation process to form the seed. Meanwhile, the
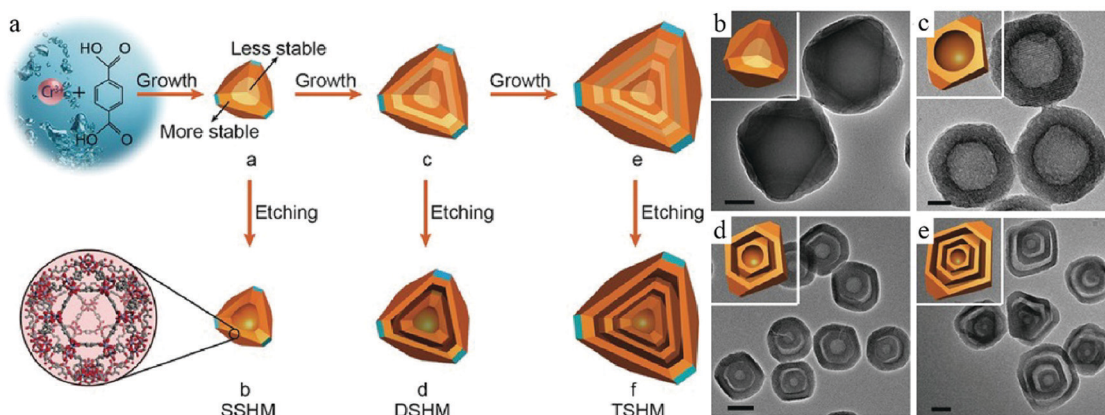

Fig. 11 (a) Fabrication of single-, double-, and triple-shelled hollow MIL-101, which are denoted as SSHM, DSHM, and TSHM, respectively. TEM images of (b) solid MIL-101, (c) SSHM, (d) DSHM, and (e) TSHM. Reproduced with permission.[38] Copyright 2017, Wiley-VCH.

Fig. 12 (a) Illustration of the hollow polymer sphere (HPS) synthesis process. (b) TEM images of HPS and (c) the corresponding elemental mappings. Reproduced with permission.[39] Copyright 2020, Royal Society of Chemistry.
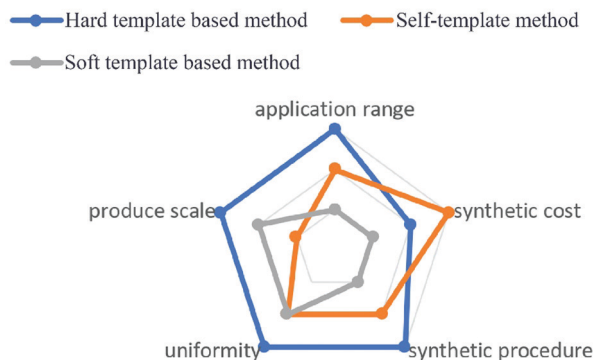

Fig. 13 Advantages and disadvantages of the three synthesis methods for HCNs.

coexistent melamine would also polymerize with diamino-benzoic acid at a slower speed, which resulted in shell formation. In this way, two parallel polymerization processes facilely formed a core–shell-type structure due to the different speeds of these two reactions, which promised a highly efficient and reliable synthesis protocol for HCNs through proper reaction control in the solution (Fig. 12).

The abovementioned methods have been commonly used to synthesize HCNs in a variety of applications according to their own merits, as shown in Fig. 13. The hard-template method requires stable and uniform templates to nanocast a designed

shell, guaranteeing the homogeneity of production, while the other two methods have a simplified synthesis procedure; however, to some extent, the size and structure were uneven because of the synthesis mechanism.

3. Applications in post LIBs

The success of LIBs continues to inspire new needs in the energy storage industry, showing ever-increasing growth in energy density and cycling life, which is not possible for the current LIB technology to guarantee. Therefore, different post LIB systems such as Li–S batteries,[40] lithium–oxygen (Li–O$_2$) batteries,[41] SIBs,[42] and PIBs[13a,43] have been developed as possible alternatives to satisfy the ever-increasing demand for energy storage. The key lies in the development of suitable electrode materials that are expected to not only carry out suitable electrochemical reactions to provide higher capacity, but also be sufficiently stable to endure extended cycles for reliable and safe use.

Below, we will summarize the applications of HCNs in different post LIB technologies. Special attention will be paid toward the structure–performance relationship so as to clarify the distinct contribution originating from the structural control of the electrode materials.

3.1 Li–S batteries

As compared to LIBs, Li–S batteries use sulfur as the electro-chemically active cathode material. The multielectron reduction process of sulfur is highly favorable to provide a high capacity of

This journal is © The Royal Society of Chemistry and the Chinese Chemical Society 2020

Mater. Chem. Front., 2020, 4, 2283–2306 | 2293

around 1675 mA h g^{-1}, while it affords low cost with regard to the resource materials; therefore, it is very popular for large-scale energy storage applications.[44] However, the applications of Li–S technique faces challenges from a series of problems.[45] First, the continuous reduction of sulfur can produce lithium polysulfides (Li$_2$S$_x$), which are easily soluble in ether-based solvents, resulting in the well-known polysulfide shuttle effect of the active species and leading to a continuous decrease in the reversible capacity. Meanwhile, large volumetric changes during the charge/discharge process as well as the insulating nature of sulfur can cause serious concerns regarding the reversibility of the reactions. Therefore, it has been a continuous pursuit to optimize the structural engineering of electrode materials, particularly carbonaceous substrates that are used to load sulfur, to not only achieve maximum sulfur utilization, but also combat the detrimental shuttle effect to improve the cycling stability of Li–S for practical use.[46]

Hollow structures are favorable choices for the structural design of electrode materials due to their capability to accommodate volumetric deformations during the charge/discharge process. The efficient role played by a hollow structure was revealed by Abruña et al., who proposed to build a PANI–sulfur yolk–shell nanocomposite as the sulfur cathode (Fig. 14).[25] PANI shell was measured to be about 15 nm, whereas the small sulfur core (∼300 nm) facilitated both ionic Li$^+$ transport and the electrochemical availability efficiency of sulfur because of its poor conductivity. The characteristic internal void provided the necessary space to tolerate volumetric changes during the reaction; therefore, the nanocomposite exhibited not only higher reversible capacity, but also much more stable cycling performance. For comparison, a control sample of a core–shell-structured S–PANI nanocomposite showed much worse electrochemical performance. The particles lacked the much-needed

buffering capability to volumetric changes and therefore were mechanically more fragile and easier to crack during the charge/discharge process, highlighting the importance of structural design in achieving the desired Li–S charge/discharge behavior.

Researchers have also identified that the mesopores of carbon can prove to be a good host for sulfur; accordingly, C–S nanocomposites with sulfur encapsulated inside the mesopores have been used as Li–S cathodes.[47] Combined with the structural engineering on the mesopores of the carbon matrix, it enabled the preparation of HCNs–S nanocomposites that could mitigate the performance degradation of Li–S batteries. For example, Wang et al. initiated a hard-template-based route for the creation of nitrogen-doped HCNs, whose carbon walls were synthesized into a mesoporous state with radially aligned pore architecture (Fig. 15).[48] The introduction of sulfur through the sublimation process resulted in the formation of the HCNs–S cathode. The authors demonstrated that such a structure could be advantageous for Li–S battery applications with different benefits. As expected, the interior cavity could effectively combat the volumetric deformation of the sulfur species. The mesopores together with their unique radially aligned configuration contributed toward good reaction kinetics with better utilization of the active species. Meanwhile, the authors proposed that nitrogen could help to anchor the soluble Li$_2$S$_x$ to further alleviate capacity fading. With all these features, the prepared HCNs–S cathode could achieve high sulfur loading of 75% and extraordinary capacity retention, which diminished the capacity loss to only 0.044% per cycle over 1000 cycles when tested at 1C.

In view of the severe damage caused by Li$_2$S$_x$ dissolution, researchers have taken painstaking efforts to trap this electrochemically active species in the cathode instead of transporting
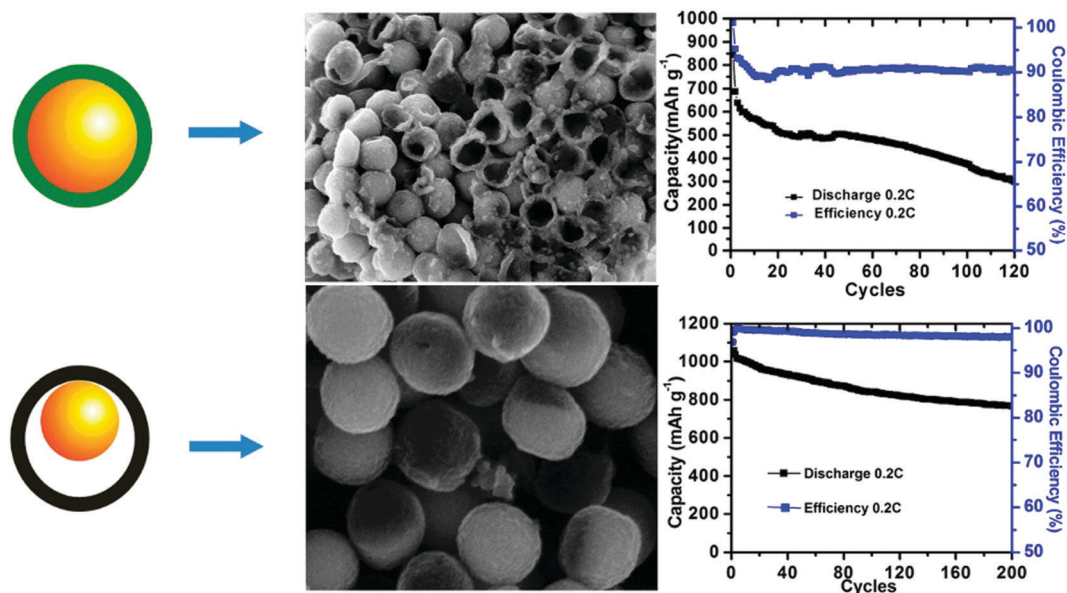

Fig. 14 Schematic comparison of the S–PANI core–shell and yolk–shell SEM images after running five cycles in cells and long-term cycling performance. Reproduced with permission.[25] Copyright 2013, American Chemical Society.

Fig. 15 (a) Fabrication processes of N-doped hollow carbon nanospheres with a tailored internal structure (TI-NHCNS). (b and c) SEM images of TI-NHCNS8 at different magnifications. (d) Rate and (e) cycling performance of the as-prepared TI-NHCNS/S cathodes. Reproduced with permission.[48] Copyright 2020, Wiley-VCH.

it to the anode for preventing capacity loss. In the regard, the introduction of an effective trapping agent that can adsorb the released Li_2S_x has become a reasonable strategy. Elemental doping, as discussed above, represents a successful treatment for C–S cathodes, which can improve the adsorption of polysulfides on the carbon matrix. Meanwhile, functional materials that can strongly adsorb polysulfides has become the favorable choice for component design of cathodes,[49] whose existence could be effectively integrated with structural control over the carbon matrix, thereby achieving the maximum effect of the materials design on the performance of Li–S batteries. For example, Lou *et al.* managed to synthesize a hollow nanocomposite of TiO@C (Fig. 16) through a step-by-step hard-template-based route.[4a] The existence of TiO was found to be critical to improve the cyclability of the Li–S battery when 550 nm TiO@C was used as the host for S. The authors identified that a 30 nm TiO shell itself was defect-rich and showed strong affinity toward Li_2S_x; accordingly, the composite shell could prevent the outward diffusion of the formed Li_2S_x. In this way, the TiO@C/S cathode showed promising electrochemical performance with a high discharge capacity of 1100 mA h g^{-1} (0.1C) as well as long cyclability with much reduced capacity fading.

Besides Li–S batteries, it should be noted that electrochemically active S can also couple with other metals for use in different battery systems, where the advantages of HCNs can also be applied. For example, Chou *et al.* demonstrated that the use of mesoporous HCNs as the sulfur host was critical to ensure the fabrication of high-performance room-temperature Na–S batteries, which was considered to be related to the unique capability of HCNs in combating the common problems of S cathodes (such as volumetric changes and polysulfide shuttle effect).[50]

3.2 SIBs

The interest in SIBs has been driven by the economic consideration as the continuous development of LIBs has raised serious concerns on the availability of lithium resources. As compared to lithium, sodium is much lower in cost and is much more evenly distributed on earth; therefore, SIBs have become an attractive and competitive candidate for applications in large-scale energy storage systems.[51] Sharing a similar working mechanism (known as rocking-chair-type batteries), SIBs have witnessed faster development in recent years from the lab to an industrial scale.[52] Borrowing knowledge from

This journal is © The Royal Society of Chemistry and the Chinese Chemical Society 2020

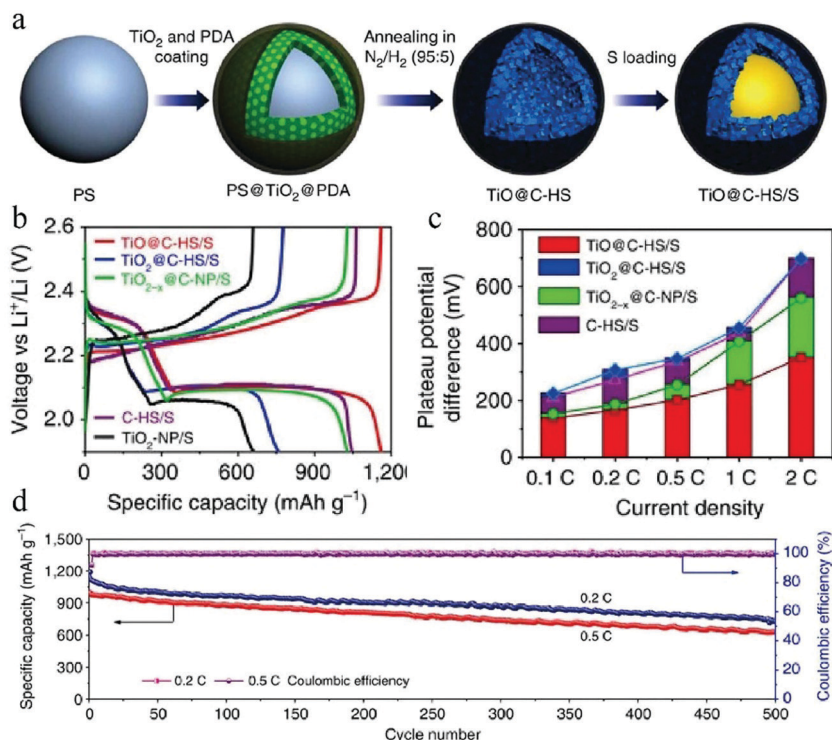*Mater. Chem. Front.*, 2020, **4**, 2283–2306 | **2295**

Fig. 16 (a) Schematic illustration of the synthesis process of the TiO@C–HS/S composite. (b) Second-cycle galvanostatic charge/discharge voltage profiles at 0.1C. (c) Potential differences between the charge and discharge plateaus at various current densities of the electrodes. (d) Prolonged cycling life and coulombic efficiency of the TiO@C–HS/S electrode at 0.2 and 0.5C. Reproduced with permission.[4a] Copyright 2016, Nature.

LIBs, researchers have been able to develop different kinds of electrode materials to test their potential in SIBs, which currently is still an essential task in the design of high-performance SIBs for their practical applications.

As compared to LIBs, one of the major challenges facing SIBs is related to the much worse stability of their electrode materials, which is related to the much larger size of Na^+ (1.02 Å) as compared to Li^+ (0.76 Å), whose continuous intercalation/deintercalation can induce large volumetric deformations; accordingly, this can easily lead to structural deformations and capacity fading of the electrode materials.[53] Meanwhile, the larger size of Na^+ can lead to much worse kinetics, which inevitably deteriorates the high rate capability of the battery. Therefore, it has become necessary that an effective stabilization mechanism be enforced on the prepared electrode materials so as to achieve satisfactory electrochemical performance. With regard to carbonaceous materials used in the anode, structural engineering is, therefore, usually employed in order to modulate the storage behavior to achieve cycling stability and high rate capability.[54] In this regard, HCNs have turned out to be a highly favored choice due to their extraordinary capability in fighting against structural deformations and improving the reaction kinetics as demonstrated in other battery systems, particularly Li–S batteries as discussed above.

Maier *et al.* were the first to use hollow-structured carbon as the anode material for SIBs.[55] Using the hard-template-based synthesis route, HCNs were prepared with a size of around 200 nm with ∼12 nm of disordered graphitic-like shell composed of ∼2–3 short carbon layers. The prepared particles showed hard carbon nature with the existence of disordered lattices resulting from the carbonization of the glucose precursor. When used as the anode material, the HCN sample showed obvious advantage with regard to both cyclability and high rate capability as compared to those of the solid particles used as the control sample (Fig. 17); this was attributed to the much lower charge transfer resistance (R_{ct}) induced by the hollow structures.
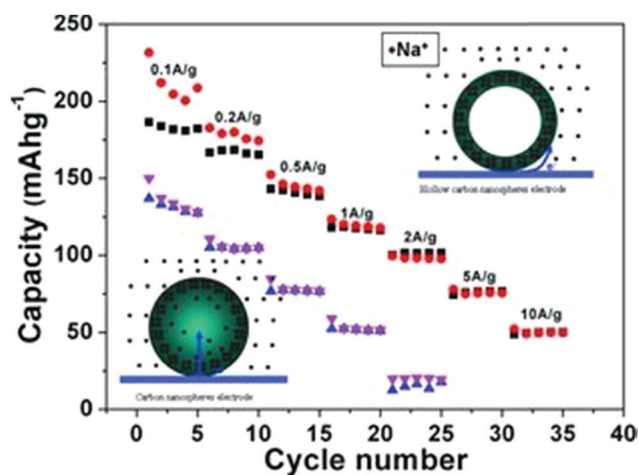

Fig. 17 Schemes of the electrochemical reaction process and realistic rate performance of HCNs and solid carbon spheres. Reproduced with permission.[55] Copyright 2012, Wiley-VCH.

The authors ascribed the improvement in the electrochemical performance particularly to the morphological control of the carbon anodes, where the large electrode/electrolyte contact and thinner wall were critical to facilitate the fast reaction kinetics during the charge/discharge process.

It should be noted that highly crystalline carbon species, particular graphite, have been known to show limited capability toward hosting Na$^+$, which has been considered to be related to the relatively narrow lattice spacing for large-sized Na$^+$ as well as the thermodynamic instability of Na-intercalated graphite compound.[56] Researchers have investigated strategies to modulate the physicochemical properties of the crystalline carbons so that they could be used in SIBs. Consequently, elemental doping has proven to be an effective strategy to achieve this

goal. For example, Zhao *et al.* synthesized HCNs (shell size: ~20–30 nm; shell wall: ~8–10 nm), whose walls existed as crystalline carbon codoped by N and S.[57] Wider lattice spacing was recorded with average interlayer spacing of 0.375 nm, which was larger than the spacing of 0.34 nm for the undoped carbon lattice (Fig. 18). The authors found that this N/S-codoped HCNs showed a reversible capacity of 448 mA h g^{-1} when tested at a current density of 100 mA g^{-1}, which was much higher than the capacity of the undoped sample (less than 200 mA h g^{-1}). Meanwhile, the N/S-HCNs sample showed extraordinary rate capability with a capacity of 169 mA h g^{-1} at a high current density of 32 000 mA g^{-1}, revealing the fast charge transport and reaction kinetics of the prepared electrodes. The authors considered that the structural control, typically the hollow feature

Fig. 18 (a) Schematic representation of S/N@C synthesis. (b) HRTEM and (c) HAADF analysis of S/N@C. (d) Cycling performance at a current density of 16 000 mA g^{-1}. Reproduced with permission.[57] Copyright 2019, Wiley-VCH.

This journal is © The Royal Society of Chemistry and the Chinese Chemical Society 2020

Mater. Chem. Front., 2020, **4**, 2283–2306 | **2297**

with a thin carbon wall, together with the codoping effect worked together to achieve highly favorable battery performance, affording both high capacity and rate capability.

Besides carbon alone as the active materials for Na$^+$ storage, the cavity of HCNs can also act as a good container to load electrode materials, thereby forming a composite material with the potential to achieve high capacity while maintaining good cycling stability. In this regard, different materials such as metal chalcogenides,[58] phosphorous,[59] and metal phosphides[60] have been introduced to integrate with HCNs so that the hollow structure could effectively buffer any volumetric changes in these materials during the charge/discharge process. A representative work could be found in the paper by Guan *et al.*, who reported the construction of a yolk–shell-structured SnS$_2$@C nanocomposite through a typical hard-template-based synthesis route.[61] As shown in Fig. 19, SnS$_2$ species were effectively encapsulated inside the carbon wall, leaving sufficient buffering room to tolerate any volumetric changes during the charge/discharge process. The author confirmed that such yolk–shell-type structure was advantageous for SnS$_2$. Much higher cycling performance was obtained with reversible discharge capacity close to 690 mA h g^{-1} after 100 cycles when tested at a current density of 0.1 A g^{-1}, highlighting the obvious advantage of electrochemically active species of SnS$_2$ in ensuring high capacity, which is partially related to the alloying capability of its reduction product, namely, Sn, to store multiple Na. The authors demonstrated that the unique structure of SnS$_2$@C including the interior void space, carbon coating, and nanosheet state of SnS$_2$ could be combined together to achieve superior performance with regard to both high capacity and cycling stability.

3.3 PIBs

PIB systems share similar operation principles as those of both LIBs and SIBs, which follow a rocking-chair mechanism based on the transportation of K$^+$ between the cathode and anode materials.[62] The increasing research attention on PIBs is also driven by the pursuit of high-energy battery made of earth-abundant materials.[63] As compared to SIBs, PIBs exhibit their own advantages toward different aspects.[64] First, K/K$^+$ has more negative redox potential as compared to Na/Na$^+$ (-2.93 V *vs.* -2.71 V; both of them are compared with respect to a standard hydrogen electrode (SHE)), which is critical to ensure high voltage for the assembled batteries. Second, K$^+$ has a smaller Stokes radius of solvated ions as compared to Na$^+$, which results in higher ion mobility in solution. Last but not least, although graphite has proven to not be a good anode material for SIBs, it has shown promising potential as a high-capacity material to store K$^+$. Therefore, it has become convenient for a possible technique transfer from LIBs to PIBs to facilitate their practical applications.

Despite the appealing merits, the development of PIBs is hindered by the availability of stable electrode materials that can sustain extended charge/discharge cycles. The even larger size of K$^+$ (1.38 Å *vs.* 0.76 Å for Li$^+$) can cause much severe volumetric changes in the host material, which has become a formidable challenge during materials design.[65] For the anode materials considered in this review, continuous volumetric deformations are known to cause an unstable solid electrolyte interphase (SEI), leading to the continuous consumption of electrolyte from the newly exposed surface of anode materials due to the emergence of cracks.[66] Such aggravated structural changes could also result in electrode pulverization and continuous capacity fading of the active materials, thereby making it imperative that effective strategies be enforced to combat the stability of electrode materials for possible practical applications.

The mechanical flexibility of a hollow structure makes it suitable to tolerate volumetric deformations.[67] Therefore, HCNs have become a favorable choice in the development of anode materials for HCNs. A recent work by Cao *et al.* clearly revealed the advantage of a hollow structure with regard to both cycling stability and rate capability when compared to a control sample of solid particles.[36] The authors used a STP to prepare hollow poly(*m*-phenylenediamine) (PmPD) by modulating the inner inhomogeneity inside the Cu–PmPD particles. The inner

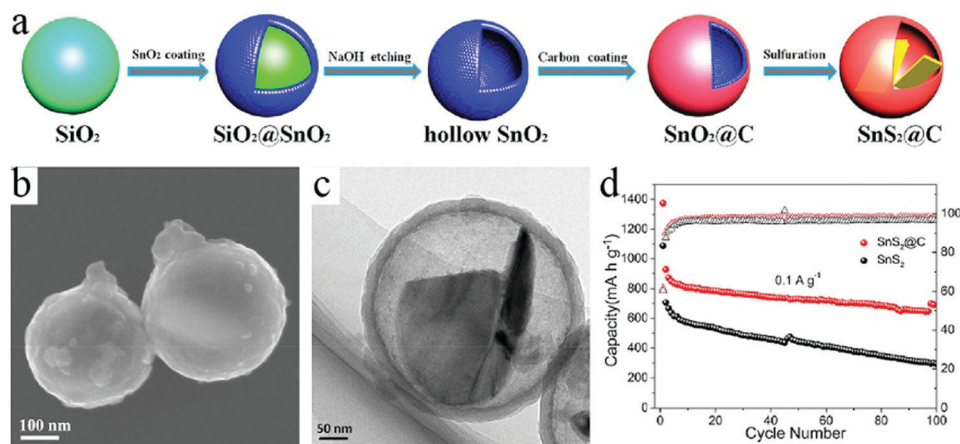Fig. 19 (a) Schematic of the formation process of SnS$_2$@C. (b) SEM and (c) TEM images of the as-prepared SnS$_2$@C. (d) Cycling performance of SnS$_2$@C electrode at current densities of 0.1 A g^{-1}. Reproduced with permission.[61] Copyright 2018, Elsevier.

2298 | *Mater. Chem. Front.*, 2020, **4**, 2283–2306

This journal is © The Royal Society of Chemistry and the Chinese Chemical Society 2020

Fig. 20 (a) Synthesis protocol for HCNs. (b) First two charge/discharge curves for HCNs at 0.1C. (c) Cycling performance and (d) rate capability of two samples, namely, HCNs and solid carbon nanospheres. (e) Electrochemical impedance of the two samples before cycling and after 100 cycles. Reproduced with permission.[36] Copyright 2020, American Chemical Society.

portion of the newly precipitated material existed as oligomers with a lower polymerization degree, which could be selectively removed to achieve the facile construction of hollow structures (Fig. 20). After the synthesis of HCNs with a cavity size of around 100 nm, they were tested as the anode material in PIBs with solid nanospheres used for comparison. The authors found that 91% of the initial reversible capacity remained after 100 cycles for the hollow sample, while this value was only 67% for those solid nanospheres, revealing the obvious advantage of HCNs in providing stable electrochemical performance. Meanwhile, the HCN sample showed much higher rate capability as well as lower charge transfer impedance than those of its solid counterpart, corresponding to a characteristic benefit from the hollow structures featuring much higher charge transportation kinetics.

It was also found that the architecture of the hollow structure also plays an important role in the K$^+$ storage capability. For example, Wan et al. could construct multishelled HCNs (MS-HCNs) with good control over the morphological characteristics and subsequently used them as anode materials for PIBs.[35] The authors proposed that the increased number of shells would lead to two adverse effects in the charge storage capability of the MS-HCN samples, namely, the surface/ interface effect beneficial for higher capability together with an increased charge transfer impedance unfavorable for K$^+$ intercalation. Accordingly, 3S-HCNs showed the best electrochemical performance when compared to the other samples (namely, 1S-HCNs and 5S-HCNs). Further, the same group successfully fabricated carbon foam whose constituent units were interconnected hollow channels with spherical knots, showing neuron-like three-dimensional architecture (Fig. 21).[68] The authors demonstrated that the interpenetrating network of the carbon scaffold was mechanically stable and flexible to tolerate volumetric deformations during the potassiation/ depotassiation process, thereby delivering a high reversible

capacity of 340 mA h g^{-1} (tested at 0.1C) as well as extraordinary cycling stability.

In addition to morphological control over the hollow structure, researchers have also tried to modulate the K$^+$ storage behavior by compositional control of the carbon materials, which has been achieved via either elemental doping[69] or integration with alloy-based high-capacity materials.[70] For example, Yang et al. found that the codoping of S and O in the carbon structures could expand their interlayer spacings to facilitate the intercalation of K$^+$.[71] A recent study by Miltin et al. demonstrated that sulfur-grafted HCNs could create C–S chemical bonds for a much higher K$^+$ storage capacity.[72] The authors used the SiO$_2$-assisted route for the creation of hollow carbon structures (diameter: ∼400 nm; thickness: 40 nm). The authors used a relatively low temperature for the carbonization process so that a higher amount of sulfur could be retained in the structures, forming a highly disordered sulfur-rich carbon matrix that could be used as the anode material for PIBs (Fig. 22). A reversible capacity of 581 mA h g^{-1} was recorded, which is much higher than both S-free HCN sample and simple mixture of S and HCNs. Although a clear storage mechanism for such an extraordinary K$^+$ storage capability was not available, the authors proposed that the coexistent S, O, and the related carbon defects were responsible for the increased capacity due to their capability to adsorb K$^+$ in a reversible manner.

During the search for high-capacity electrode materials, it has become convenient for materials scientists to integrate HCNs with alloy-based anode materials, thereby reaching their full potential toward K$^+$ storage capacity under the protection of a favorable hollow structure. Accordingly, yolk–shell-type anode materials such as CoP@C[60] and MoSe$_2$/C[73] have recently found broader use in the field of PIBs, highlighting the essential role played by concerted control over both structure and composition in the development of high-performance electrode materials.

This journal is © The Royal Society of Chemistry and the Chinese Chemical Society 2020

Mater. Chem. Front., 2020, **4**, 2283–2306 | **2299**

Fig. 21 SEM images of (a) the melamine–formaldehyde (MF) resin precursor and (b–d) the carbon product after pyrolysis. (e) Schematic of a typical neuron structure. (f) Charge/discharge curves at 0.1C for the first cycle and (g) rate capability test of the hollow interconnected neuron-like carbon architecture (HINCA)-type product in PIBs. Reproduced with permission.[68] Copyright 2018, American Chemical Society.

4. Summary

In this contribution, we have updated regarding the recent progresses made in the synthesis and applications of HCNs. Two major synthesis protocols, namely, TBRs and STPs, were discussed in detail to not only resolve the problems related to their shape control mechanisms, but also obtain a clear understanding on the capability of each synthesis route in controlling the structural features. Further, we introduced the representative applications of the prepared HCNs in different post LIB technologies, which included, but were not limited to, Li–S batteries, SIBs, and PIBs. We demonstrated that the hollow structures endowed the carbon materials with great features such as high mechanical flexibility, fast reaction kinetics, and good carrier capability, which made HCNs of particular interest in addressing critical issues related to cycling stability and rate capability, as well as facilitating their application in emerging energy storage techniques.

Despite the obvious advantages, HCNs still face enormous challenges toward their practical applications in energy storage fields. First, the development of reliable synthesis routes is still

an emergent need, which should be capable of ensuring the scalable production of HCNs with control over their structural features. The current syntheses succeeded in formulating model HCN systems available to exploit their potential, but their limited yield and complicated growth control have become a serious concern for their applications. New synthesis endeavors are expected to produce HCNs in satisfactory yield and improved quality to facilitate their usage in large-scale energy storage. Meanwhile, although structural control could make a substantial contribution to improve the cycling stability and rate capability of different batteries, the overall electrochemical performance is still far from satisfactory. In particular, the coulombic efficiency—an important parameter for batteries—is usually very low for HCN samples, which is partially related to their higher surface area. Therefore, rational structural design and component optimization are particularly important. The characteristic of high specific surface area is a double-edged sword. Appropriate cavity size and porosity are conducive to improving the electrochemical performance of the material, while they may induce marginal side-effects. In addition, the types of compound elements (such as metal/nonmetal elements)

Fig. 22 (a) Illustration of the synthesis process for sulfur-grafted HCSs. (b) CV curves, (c) galvanostatic profiles, (d) cyclability, and (e) rate performance of HCS electrodes. (f) Estimated energy density contribution of the state-of-the-art carbon-based anodes in half-cells, taking into account their position vs. the universal SHE redox potential employed as the ideal cathode. Reproduced with permission.[72] Copyright 2019, Wiley-VCH.

and the component ratios also need to be carefully optimized in practical applications. Furthermore, although it is encouraging that a theoretically high energy density for different post LIB techniques promises enormous potential, researchers still have a limited understanding regarding these systems as compared to their knowledge on LIBs. For example, the charge storage mechanism on carbon-based anodes is known to be a subject of debate for batteries such as SIBs and PIBs. There exist a large variety of models proposed to describe the interactions between hard carbon and metal cations, while a consensus on the charge storage mechanism is still lacking. Last but not least, the success of HCNs have mainly relied on the hard carbon species with a relatively low crystallization degree. Considering the decisive role played by the carbon lattice in charge storage, it is expected that the structural engineering of carbon materials could be effectively expanded into other species, particularly soft carbon and graphite, as well as be integrated with other control strategies such as compositional design to achieve optimized battery performance for different post LIB techniques.

Conflicts of interest

There are no conflicts of interest to declare.

Acknowledgements

References

1 (a) P. Simon and Y. Gogotsi, Materials for electrochemical capacitors, *Nat. Mater.*, 2008, **7**, 845–854; (b) M. F. L. De Volder, S. H. Tawfick, R. H. Baughman and A. J. Hart, Carbon Nanotubes: Present and Future Commercial

Applications, *Science*, 2013, **339**, 535; (*c*) C. Hu, M. Li, J. Qiu and Y.-P. Sun, Design and fabrication of carbon dots for energy conversion and storage, *Chem. Soc. Rev.*, 2019, **48**, 2315–2337; (*d*) J. Wang, J. Wan, N. Yang, Q. Li and D. Wang, Hollow multishell structures exercise temporal–spatial ordering and dynamic smart behaviour, *Nat. Rev. Chem.*, 2020, **4**, 159–168; (*e*) J. Zhang, F. Chen, Y. Zhao and M. Liu, Improving Elasticity of Conductive Silicone Rubber by Hollow Carbon Black, *Chem. Res. Chin. Univ.*, 2019, **35**, 1124–1132; (*f*) Y. Junjie, T. Jiayi, Z. Xiaojun, M. Liang, Z. Tingmei, N. Zheng, C. Xiangzhen, Z. Liang, J. Lin and S. Yinghui, Multi-shell Hollow FeP Microspheres as Efficient Electrocatalyst for Hydrogen Evolution at All pH Values, *Chem. J. Chin. Univ.*, 2019, **40**, 2340–2347.

2 (*a*) M. Winter, B. Barnett and K. Xu, Before Li Ion Batteries, *Chem. Rev.*, 2018, **118**, 11433–11456; (*b*) C. Yang, J. Chen, X. Ji, T. P. Pollard, X. Lü, C.-J. Sun, S. Hou, Q. Liu, C. Liu, T. Qing, Y. Wang, O. Borodin, Y. Ren, K. Xu and C. Wang, Aqueous Li-ion battery enabled by halogen conversion–intercalation chemistry in graphite, *Nature*, 2019, **569**, 245–250.

3 (*a*) J. Liu, T. Yang, D.-W. Wang, G. Q. Lu, D. Zhao and S. Z. Qiao, A facile soft-template synthesis of mesoporous polymeric and carbonaceous nanospheres, *Nat. Commun.*, 2013, **4**, 2798; (*b*) F. Xu, Z. Tang, S. Huang, L. Chen, Y. Liang, W. Mai, H. Zhong, R. Fu and D. Wu, Facile synthesis of ultrahigh-surface-area hollow carbon nanospheres for enhanced adsorption and energy storage, *Nat. Commun.*, 2015, **6**, 7221; (*c*) J. Wang, H. Tang, H. Wang, R. Yu and D. Wang, Multi-shelled hollow micro-/nanostructures: promising platforms for lithium-ion batteries, *Mater. Chem. Front.*, 2017, **1**, 414–430; (*d*) J. Wang, Y. Cui and D. Wang, Design of Hollow Nanostructures for Energy Storage, Conversion and Production, *Adv. Mater.*, 2019, **31**, 1801993.

4 (*a*) Z. Li, J. Zhang, B. Guan, D. Wang, L.-M. Liu and X. W. Lou, A sulfur host based on titanium monoxide@carbon hollow spheres for advanced lithium–sulfur batteries, *Nat. Commun.*, 2016, **7**, 13065; (*b*) J. Liu, L. Yu, C. Wu, Y. Wen, K. Yin, F.-K. Chiang, R. Hu, J. Liu, L. Sun, L. Gu, J. Maier, Y. Yu and M. Zhu, New Nanoconfined Galvanic Replacement Synthesis of Hollow Sb@C Yolk–Shell Spheres Constituting a Stable Anode for High-Rate Li/Na-Ion Batteries, *Nano Lett.*, 2017, **17**, 2034–2042.

5 (*a*) P. He, X.-Y. Yu and X. W. Lou, Carbon-Incorporated Nickel–Cobalt Mixed Metal Phosphide Nanoboxes with Enhanced Electrocatalytic Activity for Oxygen Evolution, *Angew. Chem., Int. Ed.*, 2017, **56**, 3897–3900; (*b*) P. Ge, S. Li, L. Xu, K. Zou, X. Gao, X. Cao, G. Zou, H. Hou and X. Ji, Hierarchical Hollow-Microsphere Metal–Selenide@Carbon Composites with Rational Surface Engineering for Advanced Sodium Storage, *Adv. Energy Mater.*, 2019, **9**, 1803035; (*c*) Y.-G. Sun, T.-Q. Sun, X.-J. Lin, X.-S. Tao, D. Zhang, C. Zeng, A.-M. Cao and L.-J. Wan, Facile synthesis of hollow Ti2Nb10O29 microspheres for high-rate anode of Li-ion batteries, *Sci. China: Chem.*, 2018, **61**, 670–676.

6 (*a*) Y. Fang, X.-Y. Yu and X. W. Lou, Bullet-like Cu9S5 Hollow Particles Coated with Nitrogen-Doped Carbon for Sodium-Ion Batteries, *Angew. Chem., Int. Ed.*, 2019, **58**, 7744–7748; (*b*) G. Zhang, J. Zhang, Q. Qin, Y. Cui, W. Luo, Y. Sun, C. Jin and W. Zheng, Tensile force-induced tearing and collapse of ultrathin carbon shells to surface-wrinkled grape skins for high performance supercapacitor electrodes, *J. Mater. Chem. A*, 2017, **5**, 14190–14197; (*c*) F. Wang, B. Wang, T. Ruan, T. Gao, R. Song, F. Jin, Y. Zhou, D. Wang, H. Liu and S. Dou, Construction of Structure-Tunable Si@Void@C Anode Materials for Lithium-Ion Batteries through Controlling the Growth Kinetics of Resin, *ACS Nano*, 2019, **13**, 12219–12229.

7 (*a*) G. D. Park, J.-K. Lee and Y. C. Kang, Synthesis of Uniquely Structured SnO2 Hollow Nanoplates and Their Electrochemical Properties for Li-Ion Storage, *Adv. Funct. Mater.*, 2017, **27**, 1603399; (*b*) W. Weng, J. Lin, Y. Du, X. Ge, X. Zhou and J. Bao, Template-free synthesis of metal oxide hollow micro-/nanospheres via Ostwald ripening for lithium-ion batteries, *J. Mater. Chem. A*, 2018, **6**, 10168–10175; (*c*) G. Wu, X. Liang, L. Zhang, Z. Tang, M. Al-Mamun, H. Zhao and X. Su, Fabrication of Highly Stable Metal Oxide Hollow Nanospheres and Their Catalytic Activity toward 4-Nitrophenol Reduction, *ACS Appl. Mater. Interfaces*, 2017, **9**, 18207–18214.

8 (*a*) T. Liu, L. Zhang, W. You and J. Yu, Core–Shell Nitrogen-Doped Carbon Hollow Spheres/Co3O4 Nanosheets as Advanced Electrode for High-Performance Supercapacitor, *Small*, 2018, **14**, 1702407; (*b*) S. Wang, L. Chen, X. Liu, L. Long, H. Liu, C. Liu, S. Dong and J. Jia, Fe/N-doped hollow porous carbon spheres for oxygen reduction reaction, *Nanotechnology*, 2020, **31**, 125404.

9 (*a*) J. Wu, C. Jin, Z. Yang, J. Tian and R. Yang, Synthesis of phosphorus-doped carbon hollow spheres as efficient metal-free electrocatalysts for oxygen reduction, *Carbon*, 2015, **82**, 562–571; (*b*) B. Y. Guan, L. Yu and X. W. Lou, Formation of Asymmetric Bowl-Like Mesoporous Particles via Emulsion-Induced Interface Anisotropic Assembly, *J. Am. Chem. Soc.*, 2016, **138**, 11306–11311; (*c*) M. Peer, M. Lusardi and K. F. Jensen, Facile Soft-Templated Synthesis of High-Surface Area and Highly Porous Carbon Nitrides, *Chem. Mater.*, 2017, **29**, 1496–1506.

10 C. Wang, J. Wang, W. Hu and D. Wang, Controllable Synthesis of Hollow Multishell Structured Co3O4 with Improved Rate Performance and Cyclic Stability for Supercapacitors, *Chem. Res. Chin. Univ.*, 2020, **36**, 68–73.

11 (*a*) F. Han, C. Y. Jun Tan and Z. Gao, Template-free formation of carbon nanotube-supported cobalt sulfide@carbon hollow nanoparticles for stable and fast sodium ion storage, *J. Power Sources*, 2017, **339**, 41–50; (*b*) Y. Zhang, L. Liu, L. Zhang, Y. Yu, H. Lv and A. Chen, Template-free method for fabricating carbon nanotube combined with thin N-doped porous carbon composite for supercapacitor, *J. Mater. Sci.*, 2019, **54**, 6451–6460; (*c*) Y. Ma, P. Liu, Q. Xie, G. Zhang, H. Zheng, Y. Cai, Z. Li, L. Wang, Z.-Z. Zhu, L. Mai and D.-L. Peng, Double-shell Li-rich layered oxide hollow microspheres with sandwich-like carbon@spinel@layered@spinel@carbon

2302 | *Mater. Chem. Front.*, 2020, **4**, 2283–2306

This journal is © The Royal Society of Chemistry and the Chinese Chemical Society 2020

shells as high-rate lithium ion battery cathode, *Nano Energy*, 2019, **59**, 184–196.

12 (*a*) J. W. Choi and D. Aurbach, Promise and reality of post-lithium-ion batteries with high energy densities, *Nat. Rev. Mater.*, 2016, **1**, 16013; (*b*) F. Wang, X. Wu, C. Li, Y. Zhu, L. Fu, Y. Wu and X. Liu, Nanostructured positive electrode materials for post-lithium ion batteries, *Energy Environ. Sci.*, 2016, **9**, 3570–3611; (*c*) H. Zhou, New energy storage devices for post lithium-ion batteries, *Energy Environ. Sci.*, 2013, **6**, 2256.

13 (*a*) Z. Jian, W. Luo and X. Ji, Carbon Electrodes for K-Ion Batteries, *J. Am. Chem. Soc.*, 2015, **137**, 11566–11569; (*b*) N. Yabuuchi, K. Kubota, M. Dahbi and S. Komaba, Research Development on Sodium-Ion Batteries, *Chem. Rev.*, 2014, **114**, 11636–11682.

14 (*a*) Z. Jian, Z. Xing, C. Bommier, Z. Li and X. Ji, Hard Carbon Microspheres: Potassium-Ion Anode Versus Sodium-Ion Anode, *Adv. Energy Mater.*, 2016, **6**, 1501874; (*b*) K. Kubota, M. Dahbi, T. Hosaka, S. Kumakura and S. Komaba, Towards K-Ion and Na-Ion Batteries as "Beyond Li-Ion", *Chem. Rec.*, 2018, **18**, 459–479.

15 (*a*) Y. Xie, Y. Chen, L. Liu, P. Tao, M. Fan, N. Xu, X. Shen and C. Yan, Ultra-High Pyridinic N-Doped Porous Carbon Monolith Enabling High-Capacity K-Ion Battery Anodes for Both Half-Cell and Full-Cell Applications, *Adv. Mater.*, 2017, **29**, 1702268; (*b*) D. Li, X. Ren, Q. Ai, Q. Sun, L. Zhu, Y. Liu, Z. Liang, R. Peng, P. Si, J. Lou, J. Feng and L. Ci, Facile Fabrication of Nitrogen-Doped Porous Carbon as Superior Anode Material for Potassium-Ion Batteries, *Adv. Energy Mater.*, 2018, **8**, 1802386.

16 (*a*) H.-H. Li and S.-H. Yu, Recent Advances on Controlled Synthesis and Engineering of Hollow Alloyed Nanotubes for Electrocatalysis, *Adv. Mater.*, 2019, **31**, 1803503; (*b*) S. Li, A. Pasc, V. Fierro and A. Celzard, Hollow carbon spheres, synthesis and applications – a review, *J. Mater. Chem. A*, 2016, **4**, 12686–12713; (*c*) X. L. Hui Sun, Progress in Preparation and Gas-sensing Application of Hollow Multishell Structured Materials, *Chem. J. Chin. Univ.*, 2020, **41**, 855–871.

17 (*a*) F. Böttger-Hiller, P. Kempe, G. Cox, A. Panchenko, N. Janssen, A. Petzold, T. Thurn-Albrecht, L. Borchardt, M. Rose, S. Kaskel, C. Georgi, H. Lang and S. Spange, Twin Polymerization at Spherical Hard Templates: An Approach to Size-Adjustable Carbon Hollow Spheres with Micro- or Mesoporous Shells, *Angew. Chem., Int. Ed.*, 2013, **52**, 6088–6091; (*b*) L. Peng, C.-T. Hung, S. Wang, X. Zhang, X. Zhu, Z. Zhao, C. Wang, Y. Tang, W. Li and D. Zhao, Versatile Nanoemulsion Assembly Approach to Synthesize Functional Mesoporous Carbon Nanospheres with Tunable Pore Sizes and Architectures, *J. Am. Chem. Soc.*, 2019, **141**, 7073–7080.

18 (*a*) Q. Zhang, W. Wang, J. Goebl and Y. Yin, Self-templated synthesis of hollow nanostructures, *Nano Today*, 2009, **4**, 494–507; (*b*) Z.-X. Cai, Z.-L. Wang, J. Kim and Y. Yamauchi, Hollow Functional Materials Derived from Metal–Organic Frameworks: Synthetic Strategies, Conversion Mechanisms,

and Electrochemical Applications, *Adv. Mater.*, 2019, **31**, 1804903.

19 T. Liu, L. Qu, K. Qian, J. Liu, Q. Zhang, L. Liu and S. Liu, Raspberry-like hollow carbon nanospheres with enhanced matrix-free peptide detection profiles, *Chem. Commun.*, 2016, **52**, 1709–1712.

20 (*a*) H. Tian, J. Liang and J. Liu, Nanoengineering Carbon Spheres as Nanoreactors for Sustainable Energy Applications, *Adv. Mater.*, 2019, **31**, 1903886; (*b*) L. Yu, X. Y. Yu and X. W. Lou, The Design and Synthesis of Hollow Micro-/Nanostructures: Present and Future Trends, *Adv. Mater.*, 2018, **30**, 1800939; (*c*) J. Liu, N. P. Wickramaratne, S. Z. Qiao and M. Jaroniec, Molecular-based design and emerging applications of nanoporous carbon spheres, *Nat. Mater.*, 2015, **14**, 763–774; (*d*) B. Li and H. C. Zeng, Architecture and Preparation of Hollow Catalytic Devices, *Adv. Mater.*, 2019, **31**, 1801104.

21 X. Li, J. Yu and M. Jaroniec, Hierarchical photocatalysts, *Chem. Soc. Rev.*, 2016, **45**, 2603–2636.

22 (*a*) C. Zhang, H. B. Wu, C. Yuan, Z. Guo and X. W. Lou, Confining Sulfur in Double-Shelled Hollow Carbon Spheres for Lithium–Sulfur Batteries, *Angew. Chem., Int. Ed.*, 2012, **51**, 9592–9595; (*b*) L.-F. Chen, Y. Lu, L. Yu and X. W. Lou, Designed formation of hollow particle-based nitrogen-doped carbon nanofibers for high-performance super-capacitors, *Energy Environ. Sci.*, 2017, **10**, 1777–1783; (*c*) S. L. Zhang, B. Y. Guan and X. W. Lou, Co–Fe Alloy/N-Doped Carbon Hollow Spheres Derived from Dual Metal–Organic Frameworks for Enhanced Electrocatalytic Oxygen Reduction, *Small*, 2019, **15**, 1805324.

23 Y. Liu, X.-Y. Yu, Y. Fang, X. Zhu, J. Bao, X. Zhou and X. W. Lou, Confining SnS2 Ultrathin Nanosheets in Hollow Carbon Nanostructures for Efficient Capacitive Sodium Storage, *Joule*, 2018, **2**, 725–735.

24 (*a*) O. Noonan, H. Zhang, H. Song, C. Xu, X. Huang and C. Yu, In situ Stöber templating: facile synthesis of hollow mesoporous carbon spheres from silica–polymer composites for ultra-high level in-cavity adsorption, *J. Mater. Chem. A*, 2016, **4**, 9063–9071; (*b*) H. Xu, X. Yin, M. Zhu, M. Han, Z. Hou, X. Li, L. Zhang and L. Cheng, Carbon Hollow Microspheres with a Designable Mesoporous Shell for High-Performance Electromagnetic Wave Absorption, *ACS Appl. Mater. Interfaces*, 2017, **9**, 6332–6341.

25 W. Zhou, Y. Yu, H. Chen, F. J. DiSalvo and H. D. Abruña, Yolk–Shell Structure of Polyaniline-Coated Sulfur for Lithium–Sulfur Batteries, *J. Am. Chem. Soc.*, 2013, **135**, 16736–16743.

26 F. Wu, L. Shi, D. Mu, H. Xu and B. Wu, A hierarchical carbon fiber/sulfur composite as cathode material for Li–S batteries, *Carbon*, 2015, **86**, 146–155.

27 S. Yang, Y. Zhu, C. Cao, L. Peng, W. L. Queen and W. Song, Controllable Synthesis of Multiheteroatoms Co-Doped Hierarchical Porous Carbon Spheres as an Ideal Catalysis Platform, *ACS Appl. Mater. Interfaces*, 2018, **10**, 19664–19672.

28 Y. Han, Y.-G. Wang, W. Chen, R. Xu, L. Zheng, J. Zhang, J. Luo, R.-A. Shen, Y. Zhu, W.-C. Cheong, C. Chen, Q. Peng,

D. Wang and Y. Li, Hollow N-Doped Carbon Spheres with Isolated Cobalt Single Atomic Sites: Superior Electrocatalysts for Oxygen Reduction, *J. Am. Chem. Soc.*, 2017, **139**, 17269–17272.

29 (*a*) X. Wang, J. Feng, Y. Bai, Q. Zhang and Y. Yin, Synthesis, Properties, and Applications of Hollow Micro-/Nanostructures, *Chem. Rev.*, 2016, **116**, 10983–11060; (*b*) J. Wang, J. Wan and D. Wang, Hollow Multishelled Structures for Promising Applications: Understanding the Structure–Performance Correlation, *Acc. Chem. Res.*, 2019, **52**, 2169–2178.

30 (*a*) X. Zhu, Y. Xia, X. Zhang, A. A. Al-Khalaf, T. Zhao, J. Xu, L. Peng, W. N. Hozzein, W. Li and D. Zhao, Synthesis of carbon nanotubes@mesoporous carbon core–shell structured electrocatalysts via a molecule-mediated interfacial co-assembly strategy, *J. Mater. Chem. A*, 2019, **7**, 8975–8983; (*b*) L. Zhou, Z. Zhuang, H. Zhao, M. Lin, D. Zhao and L. Mai, Intricate Hollow Structures: Controlled Synthesis and Applications in Energy Storage and Conversion, *Adv. Mater.*, 2017, **29**, 1602914.

31 C. Chen, H. Wang, C. Han, J. Deng, J. Wang, M. Li, M. Tang, H. Jin and Y. Wang, Asymmetric Flasklike Hollow Carbonaceous Nanoparticles Fabricated by the Synergistic Interaction between Soft Template and Biomass, *J. Am. Chem. Soc.*, 2017, **139**, 2657–2663.

32 F. Han, R. Wang, Y. Feng, S. Wang, L. Liu, X. Li, Y. Han and H. Chen, On demand synthesis of hollow fullerene nanostructures, *Nat. Commun.*, 2019, **10**, 1548.

33 H. Sun, Y. Zhu, B. Yang, Y. Wang, Y. Wu and J. Du, Template-free fabrication of nitrogen-doped hollow carbon spheres for high-performance supercapacitors based on a scalable homopolymer vesicle, *J. Mater. Chem. A*, 2016, **4**, 12088–12097.

34 T.-N. Gao, T. Wang, W. Wu, Y. Liu, Q. Huo, Z.-A. Qiao and S. Dai, Solvent-Induced Self-Assembly Strategy to Synthesize Well-Defined Hierarchically Porous Polymers, *Adv. Mater.*, 2019, **31**, 1806254.

35 D.-S. Bin, Z.-X. Chi, Y. Li, K. Zhang, X. Yang, Y.-G. Sun, J.-Y. Piao, A.-M. Cao and L.-J. Wan, Controlling the Compositional Chemistry in Single Nanoparticles for Functional Hollow Carbon Nanospheres, *J. Am. Chem. Soc.*, 2017, **139**, 13492–13498.

36 X.-S. Tao, Y.-G. Sun, Y. Liu, B.-B. Chang, C.-T. Liu, Y.-S. Xu, X.-C. Yang and A.-M. Cao, Facile Synthesis of Hollow Carbon Nanospheres and Their Potential as Stable Anode Materials in Potassium-Ion Batteries, *ACS Appl. Mater. Interfaces*, 2020, **12**, 13182–13188.

37 Y. J. Wong, L. Zhu, W. S. Teo, Y. W. Tan, Y. Yang, C. Wang and H. Chen, Revisiting the Stöber Method: Inhomogeneity in Silica Shells, *J. Am. Chem. Soc.*, 2011, **133**, 11422–11425.

38 W. Liu, J. Huang, Q. Yang, S. Wang, X. Sun, W. Zhang, J. Liu and F. Huo, Multi-shelled Hollow Metal–Organic Frameworks, *Angew. Chem., Int. Ed.*, 2017, **56**, 5512–5516.

39 H. Lin, W. Ye, Y. Liu, M. Liu, C. Song, H. Zhang, R. Lu and S. Zhang, Controlling solubility: a chemical approach toward preparing nitrogen-doped hollow carbon nanospheres, *J. Mater. Chem. A*, 2020, **8**, 1221–1228.

40 (*a*) A. Manthiram, Y. Fu, S.-H. Chung, C. Zu and Y.-S. Su, Rechargeable Lithium–Sulfur Batteries, *Chem. Rev.*, 2014, **114**, 11751–11787; (*b*) Z. Du, X. Chen, W. Hu, C. Chuang, S. Xie, A. Hu, W. Yan, X. Kong, X. Wu, H. Ji and L.-J. Wan, Cobalt in Nitrogen-Doped Graphene as Single-Atom Catalyst for High-Sulfur Content Lithium–Sulfur Batteries, *J. Am. Chem. Soc.*, 2019, **141**, 3977–3985.

41 (*a*) Z. Peng, S. A. Freunberger, Y. Chen and P. G. Bruce, A Reversible and Higher-Rate Li-O₂ Battery, *Science*, 2012, **337**, 563; (*b*) L. Ye, M. Liao, H. Sun, Y. Yang, C. Tang, Y. Zhao, L. Wang, Y. Xu, L. Zhang, B. Wang, F. Xu, X. Sun, Y. Zhang, H. Dai, P. G. Bruce and H. Peng, Stabilizing Lithium into Cross-Stacked Nanotube Sheets with an Ultra-High Specific Capacity for Lithium Oxygen Batteries, *Angew. Chem., Int. Ed.*, 2019, **58**, 2437–2442.

42 (*a*) P. K. Nayak, L. Yang, W. Brehm and P. Adelhelm, From Lithium-Ion to Sodium-Ion Batteries: Advantages, Challenges, and Surprises, *Angew. Chem., Int. Ed.*, 2018, **57**, 102–120; (*b*) W. Chen, X. Zhang, L. Mi, C. Liu, J. Zhang, S. Cui, X. Feng, Y. Cao and C. Shen, High-Performance Flexible Freestanding Anode with Hierarchical 3D Carbon-Networks/Fe7S8/Graphene for Applicable Sodium-Ion Batteries, *Adv. Mater.*, 2019, **31**, 1806664.

43 Y.-S. Xu, S.-Y. Duan, Y.-G. Sun, D.-S. Bin, X.-S. Tao, D. Zhang, Y. Liu, A.-M. Cao and L.-J. Wan, Recent developments in electrode materials for potassium-ion batteries, *J. Mater. Chem. A*, 2019, **7**, 4334–4352.

44 (*a*) X. Ji and L. F. Nazar, Advances in Li–S batteries, *J. Mater. Chem.*, 2010, **20**, 9821–9826; (*b*) C. Liang, L. Xin, M. Xiaotao, Z. Ding, X. Shoudong, Z. Xianxian, D. Donghong and L. Shibin, Preparation of V2O3 Hollow Spheres for Lithium Sulfur Batteries, *Chem. J. Chin. Univ.*, 2019, **40**, 1972–1978.

45 S.-Y. Li, W.-P. Wang, H. Duan and Y.-G. Guo, Recent progress on confinement of polysulfides through physical and chemical methods, *J. Energy Chem.*, 2018, **27**, 1555–1565.

46 (*a*) N. Jayaprakash, J. Shen, S. S. Moganty, A. Corona and L. A. Archer, Porous Hollow Carbon@Sulfur Composites for High-Power Lithium–Sulfur Batteries, *Angew. Chem., Int. Ed.*, 2011, **50**, 5904–5908; (*b*) A. Fu, C. Wang, F. Pei, J. Cui, X. Fang and N. Zheng, Recent Advances in Hollow Porous Carbon Materials for Lithium–Sulfur Batteries, *Small*, 2019, **15**, 1804786; (*c*) J. Zhao, M. Yang, N. Yang, J. Wang and D. Wang, Hollow Micro-/Nanostructure Reviving Lithium-sulfur Batteries, *Chem. Res. Chin. Univ.*, 2020, **36**, 313–319.

47 (*a*) H.-J. Peng, J.-Q. Huang, M.-Q. Zhao, Q. Zhang, X.-B. Cheng, X.-Y. Liu, W.-Z. Qian and F. Wei, Nanoarchitectured Graphene/CNT@Porous Carbon with Extraordinary Electrical Conductivity and Interconnected Micro/Mesopores for Lithium-Sulfur Batteries, *Adv. Funct. Mater.*, 2014, **24**, 2772–2781; (*b*) J. T. Lee, Y. Zhao, S. Thieme, H. Kim, M. Oschatz, L. Borchardt, A. Magasinski, W.-I. Cho, S. Kaskel and G. Yushin, Sulfur-Infiltrated Micro- and Mesoporous Silicon Carbide-Derived Carbon Cathode for High-Performance Lithium Sulfur Batteries, *Adv. Mater.*, 2013, **25**, 4573–4579.

48 Z. Yu, M. Liu, D. Guo, J. Wang, X. Chen, J. Li, H. Jin, Z. Yang, X. A. Chen and S. Wang, Radially Inwardly Aligned Hierarchical Porous Carbon for Ultra-Long-Life Lithium–Sulfur Batteries, *Angew. Chem., Int. Ed.*, 2020, **59**, 6406–6411.

49 (a) X. Tao, J. Wang, C. Liu, H. Wang, H. Yao, G. Zheng, Z. W. Seh, Q. Cai, W. Li, G. Zhou, C. Zu and Y. Cui, Balancing surface adsorption and diffusion of lithium-polysulfides on nonconductive oxides for lithium–sulfur battery design, *Nat. Commun.*, 2016, **7**, 11203; (b) Q. Pang, X. Liang, C. Y. Kwok and L. F. Nazar, Review—The Importance of Chemical Interactions between Sulfur Host Materials and Lithium Polysulfides for Advanced Lithium-Sulfur Batteries, *J. Electrochem. Soc.*, 2015, **162**, A2567–A2576.

50 Y.-X. Wang, J. Yang, W. Lai, S.-L. Chou, Q.-F. Gu, H. K. Liu, D. Zhao and S. X. Dou, Achieving High-Performance Room-Temperature Sodium–Sulfur Batteries With S@Interconnected Mesoporous Carbon Hollow Nanospheres, *J. Am. Chem. Soc.*, 2016, **138**, 16576–16579.

51 (a) H. Pan, Y.-S. Hu and L. Chen, Room-temperature stationary sodium-ion batteries for large-scale electric energy storage, *Energy Environ. Sci.*, 2013, **6**, 2338–2360; (b) J. Deng, W.-B. Luo, S.-L. Chou, H.-K. Liu and S.-X. Dou, Sodium-Ion Batteries: From Academic Research to Practical Commercialization, *Adv. Energy Mater.*, 2018, **8**, 1701428.

52 (a) T. Liu, Y. Zhang, Z. Jiang, X. Zeng, J. Ji, Z. Li, X. Gao, M. Sun, Z. Lin, M. Ling, J. Zheng and C. Liang, Exploring competitive features of stationary sodium ion batteries for electrochemical energy storage, *Energy Environ. Sci.*, 2019, **12**, 1512–1533; (b) Z. Yan, Q.-W. Yang, Q. Wang and J. Ma, Nitrogen doped porous carbon as excellent dual anodes for Li- and Na-ion batteries, *Chinese, Chem. Lett.*, 2020, **31**, 583–588.

53 (a) M. H. Han, E. Gonzalo, G. Singh and T. Rojo, A comprehensive review of sodium layered oxides: powerful cathodes for Na-ion batteries, *Energy Environ. Sci.*, 2015, **8**, 81–102; (b) K. Kubota and S. Komaba, Review—Practical Issues and Future Perspective for Na-Ion Batteries, *J. Electrochem. Soc.*, 2015, **162**, A2538–A2550; (c) Y.-S. Xu, J.-C. Gao, X.-S. Tao, Y.-G. Sun, Y. Liu, A.-M. Cao and L.-J. Wan, High-Performance Cathode of Sodium-Ion Batteries Enabled by a Potassium-Containing Framework of K0.5Mn0.7Fe0.2Ti0.1O2, *ACS Appl. Mater. Interfaces*, 2020, **12**, 15313–15319.

54 (a) S. Komaba, W. Murata, T. Ishikawa, N. Yabuuchi, T. Ozeki, T. Nakayama, A. Ogata, K. Gotoh and K. Fujiwara, Electrochemical Na Insertion and Solid Electrolyte Interphase for Hard-Carbon Electrodes and Application to Na-Ion Batteries, *Adv. Funct. Mater.*, 2011, **21**, 3859–3867; (b) X. Dou, I. Hasa, D. Saurel, C. Vaalma, L. Wu, D. Buchholz, D. Bresser, S. Komaba and S. Passerini, Hard carbons for sodium-ion batteries: Structure, analysis, sustainability, and electrochemistry, *Mater. Today*, 2019, **23**, 87–104.

55 K. Tang, L. Fu, R. J. White, L. Yu, M.-M. Titirici, M. Antonietti and J. Maier, Hollow Carbon Nanospheres with Superior Rate Capability for Sodium-Based Batteries, *Adv. Energy Mater.*, 2012, **2**, 873–877.

56 Y. Liu, B. V. Merinov and W. A. Goddard, Origin of low sodium capacity in graphite and generally weak substrate binding of Na and Mg among alkali and alkaline earth metals, *Proc. Natl. Acad. Sci. U. S. A.*, 2016, 201602473.

57 A. Mahmood, S. Li, Z. Ali, H. Tabassum, B. Zhu, Z. Liang, W. Meng, W. Aftab, W. Guo, H. Zhang, M. Yousaf, S. Gao, R. Zou and Y. Zhao, Ultrafast Sodium/Potassium-Ion Intercalation into Hierarchically Porous Thin Carbon Shells, *Adv. Mater.*, 2019, **31**, 1805430.

58 P. Liu, J. Han, K. Zhu, Z. Dong and L. Jiao, Heterostructure SnSe2/ZnSe@PDA Nanobox for Stable and Highly Efficient Sodium-Ion Storage, *Adv. Energy Mater.*, 2020, 2000741.

59 H. Jin, H. Lu, W. Wu, S. Chen, T. Liu, X. Bi, W. Xie, X. Chen, K. Yang, J. Li, A. Liu, Y. Lei, J. Wang, S. Wang and J. Lu, Tailoring conductive networks within hollow carbon nanospheres to host phosphorus for advanced sodium ion batteries, *Nano Energy*, 2020, **70**, 104569.

60 Q. Liu, Z. Hu, Y. Liang, L. Li, C. Zou, H. Jin, S. Wang, H. Lu, Q. Gu, S.-L. Chou, Y. Liu and S.-X. Dou, Facile Synthesis of Hierarchical Hollow CoP@C Composites with Superior Performance for Sodium and Potassium Storage, *Angew. Chem., Int. Ed.*, 2020, **59**, 5159–5164.

61 X. Li, Y. Zhao, Q. Yao and L. Guan, Encapsulating SnS2 nanosheets into hollow carbon sphere: A yolk-shell SnS2@C composite with enhanced sodium storage performance, *Electrochim. Acta*, 2018, **270**, 1–8.

62 W. Zhang, Y. Liu and Z. Guo, Approaching high-performance potassium-ion batteries via advanced design strategies and engineering, *Sci. Adv.*, 2019, **5**, eaav7412.

63 (a) H. Kim, J. C. Kim, M. Bianchini, D.-H. Seo, J. Rodriguez-Garcia and G. Ceder, Recent Progress and Perspective in Electrode Materials for K-Ion Batteries, *Adv. Energy Mater.*, 2018, **8**, 1702384; (b) W. Zhang, W. K. Pang, V. Sencadas and Z. Guo, Understanding High-Energy-Density Sn4P3 Anodes for Potassium-Ion Batteries, *Joule*, 2018, **2**, 1534–1547; (c) B. Xu, S. Qi, F. Li, X. Peng, J. Cai, J. Liang and J. Ma, Cotton-derived oxygen/sulfur co-doped hard carbon as advanced anode material for potassium-ion batteries, *Chin. Chem. Lett.*, 2020, **31**, 217–222.

64 W. Luo, J. Wan, B. Ozdemir, W. Bao, Y. Chen, J. Dai, H. Lin, Y. Xu, F. Gu, V. Barone and L. Hu, Potassium Ion Batteries with Graphitic Materials, *Nano Lett.*, 2015, **15**, 7671–7677.

65 (a) J. C. Pramudita, D. Sehrawat, D. Goonetilleke and N. Sharma, An Initial Review of the Status of Electrode Materials for Potassium-Ion Batteries, *Adv. Energy Mater.*, 2017, **7**, 1602911; (b) Y. Liu, Y.-X. Lu, Y.-S. Xu, Q.-S. Meng, J.-C. Gao, Y.-G. Sun, Y.-S. Hu, B.-B. Chang, C.-T. Liu and A.-M. Cao, Pitch-Derived Soft Carbon as Stable Anode Material for Potassium Ion Batteries, *Adv. Mater.*, 2020, **32**, 2000505.

66 W. Zhang, J. Mao, S. Li, Z. Chen and Z. Guo, Phosphorus-Based Alloy Materials for Advanced Potassium-Ion Battery Anode, *J. Am. Chem. Soc.*, 2017, **139**, 3316–3319.

67 Z. Zhang, B. Jia, L. Liu, Y. Zhao, H. Wu, M. Qin, K. Han, W. A. Wang, K. Xi, L. Zhang, G. Qi, X. Qu and R. V. Kumar, Hollow Multihole Carbon Bowls: A Stress–Release

Structure Design for High-Stability and High-Volumetric-Capacity Potassium-Ion Batteries, *ACS Nano*, 2019, **13**, 11363–11371.

68 D.-S. Bin, X.-J. Lin, Y.-G. Sun, Y.-S. Xu, K. Zhang, A.-M. Cao and L.-J. Wan, Engineering Hollow Carbon Architecture for High-Performance K-Ion Battery Anode, *J. Am. Chem. Soc.*, 2018, **140**, 7127–7134.

69 (*a*) W. Zhang, Z. Cao, W. Wang, E. Alhajji, A.-H. Emwas, P. M. F. J. Costa, L. Cavallo and H. N. Alshareef, A Site-Selective Doping Strategy of Carbon Anodes with Remarkable K-Ion Storage Capacity, *Angew. Chem., Int. Ed.*, 2020, **59**, 4448–4455; (*b*) Y. Wu, S. Hu, R. Xu, J. Wang, Z. Peng, Q. Zhang and Y. Yu, Boosting Potassium-Ion Battery Performance by Encapsulating Red Phosphorus in Free-Standing Nitrogen-Doped Porous Hollow Carbon Nanofibers, *Nano Lett.*, 2019, **19**, 1351–1358.

70 Z. Yi, Y. Qian, J. Tian, K. Shen, N. Lin and Y. Qian, Self-templating growth of Sb2Se3@C microtube: a convention-alloying-type anode material for enhanced K-ion batteries, *J. Mater. Chem. A*, 2019, **7**, 12283–12291.

71 M. Chen, W. Wang, X. Liang, S. Gong, J. Liu, Q. Wang, S. Guo and H. Yang, Sulfur/Oxygen Codoped Porous Hard Carbon Microspheres for High-Performance Potassium-Ion Batteries, *Adv. Energy Mater.*, 2018, **8**, 1800171.

72 J. Ding, H. Zhang, H. Zhou, J. Feng, X. Zheng, C. Zhong, E. Paek, W. Hu and D. Mitlin, Sulfur-Grafted Hollow Carbon Spheres for Potassium-Ion Battery Anodes, *Adv. Mater.*, 2019, **31**, 1900429.

73 W. Wang, B. Jiang, C. Qian, F. Lv, J. Feng, J. Zhou, K. Wang, C. Yang, Y. Yang and S. Guo, Pistachio-Shuck-Like MoSe2/C Core/Shell Nanostructures for High-Performance Potassium-Ion Storage, *Adv. Mater.*, 2018, **30**, 1801812.